Universitat Rovira i Virgili

Escola Tècnica Superior d'Enginyeria Química

Revamping of an existing Pressure Swing Adsorption unit to maximize hydrogen production

Master thesis presented by Clara Weber Torres
to obtain the Master's degree in Chemical Engineering from the Universitat Rovira i Virgili

Company Supervisor: Robert Fortuny
URV Tutor: Pere Gabarra

Tarragona, February 2023

Acknowledgments

I would like to start acknowledging Pere Gabarra, the General Manager of Basf Sonatrach Propanchem, for giving me the opportunity to carry out the internship within the company as well as the present project as my Master's thesis.

I would also like to thank my company supervisor Robert Fortuny, Process Engineer within the company, for training me and giving me the opportunity to carry out tasks among the production department, as well as providing ideas and constructive feedback to make the most of this project with the time available.

Also, I would like to thank Jordi Figueras, Technology Manager within the company, for opening the way for me to work close to the plant's production personnel and see the day-to-day life of the production plant.

I owe all of the BSP personnel for providing help whenever I asked for it, for involving me in diverse supporting tasks that helped me learn and entertain myself with my leaning towards problem solving, and for always considering me one of their own from the first day I started the internship.

Thanks to all my family and friends, for their unconditional support throughout everything.

Index

Nomenclature

BSP. -	Basf Sonatrach Propanchem
PDH. -	Propane Dehydrogenation
SHP. -	Selective Hydrogenation of Propadiene
CCR. -	Continuous Catalyst Regeneration
PSA. -	Pressure Swing Adsorption
TG. -	Tail Gas
CV.-	Valve Coefficient

List of figures

List of tables

Summary

The following Master thesis report contains all of the information about the academic project *Revamping of an Existing Pressure Swing Adsorption Unit to Maximize Hydrogen Production* carried out during an internship with the company Basf Sonatrach Propanchem, S.A. The present document intends to be evaluated by the members of the jury regarding the approached problem. It additionally includes the information about the student's role within the company, to be evaluated as well by both tutors.

A brief description of the overall plant process is firstly provided with the intention of giving context to the project. Then, a preliminary introduction of the assessed Pressure Swing Adsorption unit as well as the scope of the project are defined, followed by the work placement description including the student's developed tasks during the internship.

The approach methods using the *Aspen Adsorption* software are then explained, including a description of the adsorbent bed model together with the approximations made, as well as the explanation on the different configurations considered. These included a preliminary, more theoretical simulation of adsorption breakthrough curves, along with a simulation of the existing 4-bed PSA unit taking into consideration the present constraints. Then, diverse simulations were carried out considering several hypotheses, including: a feed pressure increase, a feed pressure increase plus a change in the PSA configuration involving an extra valve manifold, a six-bed configuration, and a six-bed configuration plus a feed pressure increase.

Afterwards, an analysis of the simulated adsorption breakthrough curves is performed, as well as the model validation considering the simulation of the current PSA unit. Once this was done, results could also be withdrawn from the different hypothetical simulations, which served to evaluate the overall performance of each PSA design.

The configuration that provided the most attractive results regarding the maximization of hydrogen production was then assessed with the aim of providing a preliminary revamping case. Once the necessary assets were known, an economic estimation could be made, as well as a brief viability study. This was then compared to both the current PSA case and to an existing conceptual-phase project involving the commissioning of an entirely new PSA unit with an increased feed capacity.

The overall work described in the present document can finally serve as a starting point to evaluate different potential approaches for the functioning and optimisation of any evaluated PSA unit configuration using the *Aspen Adsorption* tool, given the future possibility that would allow the propane dehydrogenation plant to make hydrogen a main product together with propylene.

1. INTRODUCTION

BASF Sonatrach Propanchem, S.A. (from now on BSP) is a joint venture between the companies BASF and Sonatrach that produces propylene by means of the catalytic dehydrogenation of propane in the Propane Dehydrogenation plant (from now on PDH) located in La Canonja (Tarragona).

The overall process can be divided and summarised into six different sections: The feed treatment, the reactors, the separation section, the SHP section, the fractionation section and the CCR section, as outlined in Figure 1. 1.

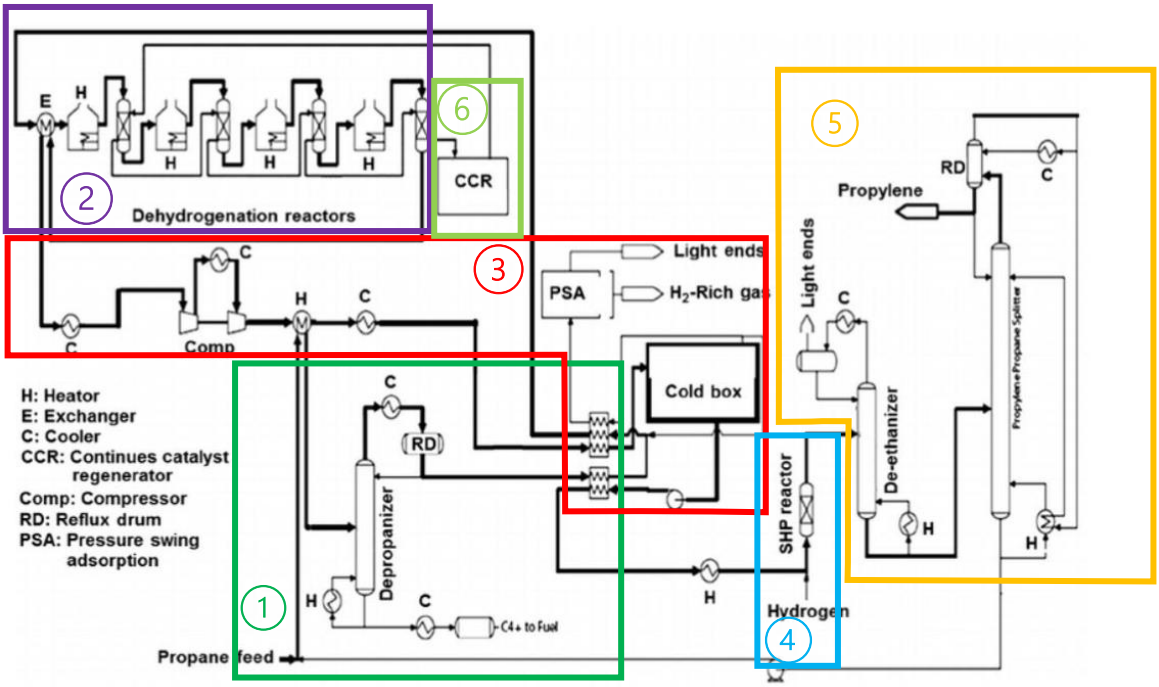

Figure 1. 1. Overall Propane dehydrogenation process of the PDH plant

1. Feed treatment section. This section is destined to separate nitrogen compounds, heavy metals (i.e. mercury) and water from the fresh propane feed. The mercury attacks the aluminium from the plate exchangers in the product separation section, while the nitrogen forms ammonium chloride in the process conditions that condenses in the reactor effluent compressor. It is also important to dry as most as possible the feed since extremely low temperatures can appear in determined sections of the process where freezing must be avoided.
2. Reactors section. In this section, the selective dehydrogenation of propane into propylene is carried out by means of a catalytic moving bed where the gas feed radially passes through, from the inner screen to the outer screen. A small quantity of other hydrocarbons is generated, mainly methane and ethane. The conditions that favour the endothermic reaction are that of low pressures and high temperatures, and the process consists of 4 reactors and 4 heaters installed in series.
3. Separation section. In the separation section, the propane is refrigerated by means of a heat exchange with the liquid product, and then mixes with recirculated cryogenic hydrogen to obtain the combined feed. Then, the reactor effluent undergoes a heat exchange with this combined feed stream, obtaining a separation

into two different streams: a gas stream rich in hydrogen, part of which is sent to the hydrogen purification unit by Pressure Swing Adsorption and a liquid product stream rich in hydrocarbons.

4. Selective Hydrogenation of Propadiene (SHP) section. In the reactor section, propadiene is formed and it is later selectively hydrogenated into propylene with a conversion of practically 100%.
5. Fractionation section. This section is destined to meet the requirement of a >99.5% purity in propylene for the product stream. Firstly, ethane and other light components are removed in the de-ethanizer, and the bottom product stream is then sent to the Propylene-Propane splitter, where propylene is obtained as the distilled component and propane is recirculated back into the process.
6. Continuous Catalyst Regeneration (CCR) section. This section has two distinctive functions: the transfer and the regeneration of the catalyst. The transfer of the catalyst is ensured to be carried out in a safe and completely controlled manner from a hydrogen/hydrocarbon atmosphere into an oxygen rich atmosphere. The regeneration of the catalyst is done by means of burning the coke, re-establishing the catalyst's activity, selectivity and stability.

Propylene has historically been the main product of the PDH plant. The resulting hydrogen from the process is recovered in a Pressure Swing Adsorption unit (from now on PSA), and it is completely utilized inside the plant's process.

Hydrogen holds a promising potential to achieve a near-zero greenhouse gas emission when used as a fuel, since it would only have water vapour emissions. It is for this main reason that hydrogen has gained prominence in the recent years, especially in the industrial sector.

The company is now aiming towards also making hydrogen a main product. That is, there ought to be a maximization of the recovery and subsequent surplus production of hydrogen to cover the plant's needs whilst also exporting part of it to third parties.

Based on adsorption theory, increasing the operating pressure of the unit could result in one of the key solutions to this issue, since pressure favours the adsorption of unwanted gases and hydrogen possesses a very low affinity to the adsorbent agents. Also, based on the working method of a PSA unit, a system with an increased number of adsorbent vessels could also maximize the hydrogen production, as it would allow to increase recovery by working with a zero idle time operation.

The proposed solution that will be developed along the present document is to simulate and validate the existing PSA unit, and later modify certain process conditions and configurations to see the change in the primary performance indicators, which are mainly hydrogen recovery and purity.

2. SCOPE OF THE PROJECT AND SPECIFIC OBJECTIVES

The main objective of the project is to study certain effects on the PSA performance by means of a numerical simulation, in order to determine the necessary revamping of the existing unit that would allow an excess flowrate of high purity hydrogen to be sold as a product to third parties. This revamping will then be economically assessed and compared to a project that involves the commissioning of an entirely new PSA unit.

The focus of the project will therefore be on this unit, which is the part of the separation section of the process dedicated to the purification of hydrogen, currently obtaining a stream with a hydrogen purity of _% (molar based) that is sent back to the process, where it is completely utilized. The aim is to maximize the production of hydrogen to supply it as a product, recovering the most of the PSA's feed stream whilst maintaining the required purity specification set by the third parties interested in the product (_ % molar based regarding hydrogen and no more than _ppm-v of carbon monoxide). The current hydrogen recovery is at approximately _%, meaning that only that percentage of the total mass of hydrogen fed into the system is recovered as a high purity stream. Hence, if the recovery is increased the purified hydrogen flowrate would be higher than the one internally required by feeding the same flowrate into the PSA, so the excess would be destined to the selling of hydrogen to third parties.

The limitations for the performance of the PSA unit were decided to be studied upon a numerical simulation model using the Aspen Adsorption™ software, which allows to simulate, analyse, and optimise industrial gas adsorption processes dynamically.

2.1. PSA Process description

The Pressure Swing Adsorption operation process is based on the concept that adsorbents have higher adsorption capacity as the gas partial pressure increases. As the conditions favour closing into the dew point, the adsorbent captures the less-volatile compounds. Therefore, when an adsorption bed operates at high pressures, the adsorbent agent will capture as most impurities as possible (depending on their affinity to the adsorbent) as it systematically saturates, losing its adsorption capacity. Hence, after a defined time period, the operating pressure is decreased so that the previously adsorbed impurities will desorb, and the adsorbent bed can later be repressurized and fed again through a series of required steps.

PSA is a commonly utilized process for hydrogen purification due to its relatively low affinity (as it constitutes a highly volatile and low polarity compound) to the adsorbent agents, allowing the obtention of high purity hydrogen streams, whilst also obtaining the denominated "Tail-gas" stream that contains the desorbed components together with the non-recovered fraction of hydrogen and is commonly used as a fuel gas.

In the case of the PDH plant's PSA unit, each of the adsorbent beds is constituted by two different layers of an adsorbent agent. The lower layer is made of activated carbon (supplied by *Calgon Carbon Corporation*), and the upper layer is constituted by molecular sieve grade 522 (also known as Zeolite 5A, supplied by *W.R. Grace and Co.*), which has proven to have a stronger adsorption towards carbon monoxide than activated carbon.

The process is semi-batch type, as it requires a dynamic operation where the arrangement of the different valves allow the control system to operate the beds accordingly. Having continuous feed, product and tail gas streams implies that the system must have multiple adsorbent beds so that there is always at least one adsorbent bed going through the adsorption step whilst the remaining beds are going through the different

regeneration steps. In the case of the PDH plant's PSA unit, it consists of a 4-bed system as the one shown in Figure 2. 1.

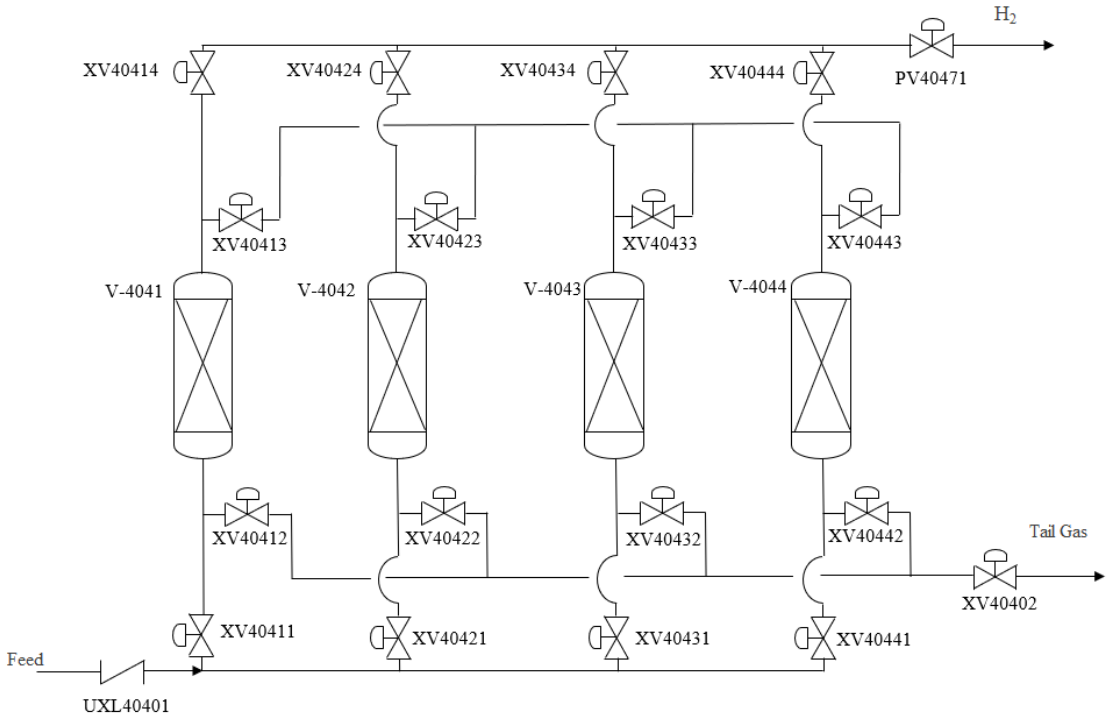

Figure 2. 1. Simplified scheme of the PSA unit in the PDH plant

All of the system's valves are automatic, with the inlet valve (UXL-40401) being an on/off valve, as well as the inlet and the tail gas valves of each bed (XV-404X1 and XV-404X2, respectively). The rest of the unit's valves have a control actuation with an equal percentage aperture pattern.

The system operates following a sequence of 12 steps cyclically, divided in four phases (one for each bed) of three steps. Figure 2. 2 shows a summary of the different steps that each of the four beds in the system goes through, which are briefly described hereunder.

	Phase nº											
	1			2			3			4		
	Step nº											
Bed	1	2	3	4	5	6	7	8	9	10	11	12
V-4041	AD			PP	BD		RP	I		P		AD
V-4042	P			AD			PP	BD		RP	I	P
V-4043	RP	I		P			AD			PP	BD	
V-4044	PP	BD		RP	I		P			AD		

Figure 2. 2. Current sequence of the PSA unit.

Adsorption step (AD): The feed stream (called net gas) is fed into the bed at the high operating pressure, which corresponds to 5,5 bar_g in the case of the present unit. Hydrogen passes through the vessel upwards (co-currently) without practically being adsorbed compared to the other components (essentially methane and carbon monoxide). Thus, the feed and product valves are completely open during this step (XV-404X1 and XV-

404X4). When the bed reaches its maximum adsorbent capacity, the feed will be switched to the next vessel.

Provide Purge step (PP): The bed is depressurized from the product side (top) co-currently, but instead of going into the H_2 collector line, the high purity hydrogen stream is now fed back into the system to purge another vessel (XV-404X3 opens completely).

Blowdown step (BD): Up until this point, the adsorbent bed has been saturated, hence the majority of the adsorbed gas components have travelled to the top of the vessel. The bed is thus further depressurized from the feed side (bottom of the vessel) counter-currently (XV-404X2 opens completely, as well as XV-40402), forcing the adsorbed components to migrate downwards into the tail gas collector pipe. The bed is depressurized down until it equalizes the tail gas pressure (0,3 bar_g).

Receive Purge step (RP): The vessel is further regenerated counter-currently by means of a high purity hydrogen stream coming from the vessel that is undergoing the Provide Purge step (XV-404X3 is regulated and XV404X2 is kept open), further dragging the adsorbed components together with hydrogen into the Tail Gas stream with the controlled action of XV-40402, hence the bed is slightly repressurized.

Idle step (I): The idle time is the wait time required to compensate the time differences between the cycle steps. All the valves are kept closed during this step.

Re-pressurization step (P): The adsorbent bed is then repressurized via high purity hydrogen from a split stream of product coming from the vessel undergoing the Adsorption step (XV404X4 is regulated). Once the maximum adsorption pressure is reached, the vessel starts the cycle over again from the Adsorption step.

Each of the cycle steps has a time defined in the control system of the unit. Adsorption time corresponds to 70 seconds (excluding the overlap band, marked with a dashed line above), which would be equivalent to the re-pressurization step time. The total cycle time is the time that one bed takes to complete an entire cycle, which is equal to the time necessary for all of the beds to undergo the adsorption step. Therefore, it can be calculated as 4 times (4 beds) 70 seconds, 240 seconds of total cycle time. The other step times are also defined within the control system: Both Provide and Receive Purge steps last 50 seconds, Blowdown lasts 20 seconds and the Idle time is set to 15 seconds. By fitting these defined step times into the scheme presented in Figure 2. 1, it is inferred that $t_1 = t_4 = t_7 = t_{10} = 50$ s, $t_2 = t_5 = t_8 = t_{11} = 15$ s, and $t_3 = t_6 = t_9 = t_{12} = 5$ s.

The PDH plant's PSA unit generally feeds an average of _ kg/h of net gas and yielding a product stream of around _ kg/h of high purity hydrogen, whilst the temperature of the feed stream is about 25 ºC and the overall PSA system, although not isothermal, doesn't have large temperature variations.

It is worth noting that the actual net gas that is fed into the PSA system has the composition presented in Table 2. 1, based on Start of Run conditions.

Table 2. 1. Actual Net gas composition at the PSA feed. *

Actual Net gas composition (molar %)						
Carbon monoxide	Ethane	Ethylene	Methane	Propane	Propylene	Hydrogen
_	_	_	_	_	_	_

*The values have been extracted from average data corresponding to the last two weeks of May 2022, as the plant worked at its full capacity.

With the specified composition, the average of _kg/h at the feed corresponds to _kmol/h. Knowing that the recovered hydrogen has a purity of _% molar-based and the

product molar flowrate is practically _ kmol/h, the hydrogen recovery is estimated to a value of _%.

Nonetheless, the intended numerical simulation for this project needs parameters that depend on applied adsorbents and process conditions that must be determined experimentally for the definition of adsorption equilibrium and kinetics in the model. Due to limitations from consistent experimental data, it has been decided that the main components that are most worth including in the simulation's system are downright hydrogen, methane, and carbon monoxide, as the first two are the most predominant and the later has a specification for the product, being that it must not exceed the limit of _ ppm-v. This is also supported by the fact that the other components present in the mixture are much minoritarian in addition to have a higher adsorption force than carbon monoxide and methane, meaning they will be even easier adsorbed, as seen in Figure 2. 3.

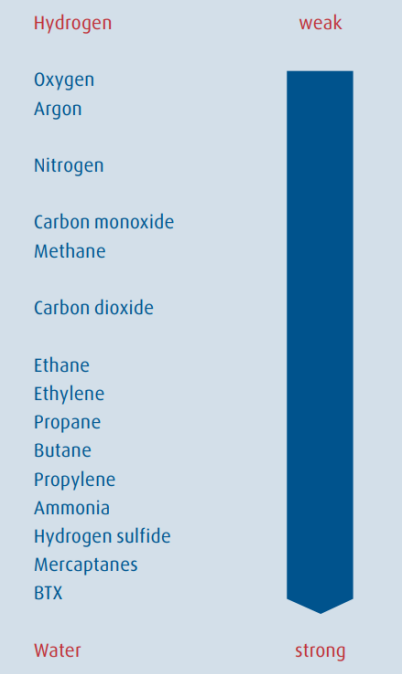

Figure 2. 3. Adsorption affinity diagram according to *Linde*. [1]

Therefore, by normalizing the molar composition values of Table 2. 1, the input of the numerical simulation will have the values presented in Table 2. 2 for the feed composition.

Table 2. 2. Net gas composition for the numerical simulation herein.

Normalized net gas composition (molar fraction)		
Carbon monoxide	Methane	Hydrogen
_	_	_

2.2. Influence of process parameters and limitations

The feed gas composition doesn't have a significant impact on a PSA process performance, and generally only feed gases that contain hydrogen in a volume proportion of less than the 50% are not economically viable for a PSA system.[2]

High purities of hydrogen are obtainable and theoretically not limited, since desired purity can be maintained due to hydrogen's low affinity to the adsorbent agents and considering the adsorbent bed vessel has a sufficient height to keep the adsorption front of impurities out of the product stream in addition to the adsorption step times being accordingly estimated and programmed. Nevertheless, it must be taken into consideration that generally, in exchange to a less restricted product specification, a higher recovery can be achieved by adjusting the cycle step times (i.e., enlarging the adsorption phase time).

Regarding recovery, it is not possible to achieve a value of a 100% in a PSA system, as part of hydrogen product is discarded through the tail gas stream together with the desorbed impurities during both the purge and blowdown steps. In a PSA system, a high feed gas pressure is generally preferred for higher hydrogen recovery values. The product pressure is usually about 0,5 bar lower than that of the feed, so the pressure drop is minor. Tail gas pressure, however, does have influence in hydrogen recovery. The lower its value, the higher is the pressure gap in the oscillations, favouring the adsorption process as described in section 2.1. Increasing the number of beds is also an option to consider, especially if both the unit's working pressure and capacity ought to be augmented. A greater number of beds allows the programming of a larger number of bed-to-bed pressure equalization steps (provide and receive purge steps), which subsequently results in a zero idle time and hence an improvement in hydrogen recovery.

A summary of the influencing parameters in a PSA system's performance, mainly indicated by hydrogen recovery and purity, is shown in Table 2. 3. [3]

Table 2. 3. Main influencing parameters on the performance of a PSA system.

	Recovery	Purity
Adsorption pressure ↑	Increase	Decrease
Equalization steps ↑	Increase	Decrease
Adsorption time ↑	Increase	Decrease

2.3. Defined specific objectives of the project

Taking into consideration all of the above, the present project aims to simulate the existing PSA unit and later modify the system according to the most affecting factors presented, by taking into consideration that the recovery of the system has to be maximized whilst having the least possible impact in product purity by maintaining the required specification (≥ _% molar in hydrogen and ≤ _ppm-vol in carbon monoxide).

In order to do so, the posterior simulations to that of the base model will include:

- Increasing the feed pressure to have a wider oscillation between the feed (adsorption) and the tail gas (desorption).
- Increasing the number of pressure equalization steps, considering that there exists an upper limit since there is a minimum hydrogen purge needed to

discard the desorbed components. This can be done by adding both valve manifolds and additional adsorbent vessels.

- Adjusting adsorption time for each approached case to have a product under specification in every simulation. There also exists a margin for the trial and error regarding valve coefficients. Hence, cycle step times and valve coefficients will both be adjusted parameters for the product purity control under a specific reference feed flowrate.

Regarding the possibility of increasing the adsorption pressure, it was primarily checked that the existing vessels can indeed work at higher pressures. Their design pressure is that of _ bar_g, and the highest adsorption pressure that will be tested during the project will not exceed _ bar_g. This is based upon an internal reference study carried out by *UOP Honeywell*.

With respect to the testing of an increased number of pressure equalization steps, it is primarily considered to add an extra pressure equalization valve manifold to the existing four-bed system. Furthermore, the addition of two extra vessels in order to change the system to a six-bed PSA unit is later tested, as this configuration allows two more pressure equalization steps per bed.

Therefore, the present project is summarised to the following key objectives:

- Building a numerical model of the existing adsorbent beds.
- Studying the breakthrough curves of the implied components in order to estimate appropriate adsorption times and further recognise the importance of the sequence arrangement.
- Simulating and validating a four-bed PSA system at the existing process conditions.
- Testing a four-bed PSA system with an increased adsorption pressure.
- Testing a six-bed PSA system with the current operating pressure.
- Testing a six-bed PSA system with an increased adsorption pressure.
- Evaluate the best possible solution by aiming towards the maximization of hydrogen recovery whilst keeping the system under the required specification.
- Estimate the necessary equipment for the evaluated revamp of the existing unit and approximate an economic assessment that compares its payback and earnings with respect to a suggested commissioning of an entirely new PSA unit with increased capacity.

The time schedule of the specific tasks planned for the project, as well as the actual time schedule carried out once the project was finished, can be consulted in Appendix A.

3. STUDENT'S ROLE IN THE COMPANY

The main role of the student at the company throughout the internship entail both the elaboration of the present project combined with diverse tasks to support the different production departments, and especially reporting to the Process department, as the internship was carried out under the supervision of the Process Engineer *Robert Fortuny*.

Initially, the student underwent a period of time dedicated especially to the learning of the process via an existing manual of the *Oleflex* technology by *UOP Honeywell* together with initial training on workplace hazards as well as access to both technical documentation and real-time visualization of displays of the process. This initial learning was also combined with preliminary support tasks related to the PSA project. The technology and process department was then in the preliminary phase of a project that involved a new PSA unit with increased capacity, and the student had the opportunity to provide with process data that had been recapped and normalised accordingly, such as certain stream averaged flowrates together with their composition, material balances, process conditions and technical documentation. This helped both further understand the PSA unit's process, recap useful information for the present project and the familiarization with the *PI ProcessBook* software, which is a display of the plant's process linked to the actual Displayed Control System that allows either direct or calculated data export to *Microsoft Excel* for the sake of a customised data use and visualization.

Other support tasks unrelated to the PSA unit were also carried out. These included the recompilation and normalisation of the newly implemented industrial chromatograph. The system provides with real-time data calculations in the reactors section, where for both the inlet and the outlet streams of each of the four reactors arranged in series there are measurements of temperature, pressure, composition, and volumetric flowrates. The velocity of the fluid at both the inlet elbow and the outlet nozzle, as well as in the inlet and outlet ring areas, was also calculated with the help of technical information. Later, the velocity of the gas mixture that passes radially from the inner to the outer screen containing the catalyst was also estimated, as well as the velocity of sound at the inlet and outlet of each reactor [4]. This information was reported to the Mechanical Asset Management team.

Other tasks involving the recompilation of information were carried out reporting to both the process team and the plant laboratory team, such as a summary of position indicators for the valves located below each catalyst collector in the continuous catalyst regeneration section for the sake of a propane intake reduction, the update of technical data for the *Oleflex* reactors after their revamp, as well as the research of the metal composition from the materials that constituted the new equipment in addition to the independent research on metal sulfide equilibria. The later resulted from a change in the operating conditions of the reactors section that were suspected to produce an increased scale formation.

The student also carried out tasks related to basic engineering calculations, mostly being reported to the technology and process engineering team. These included the estimation and rating of CVs to preliminary estimate whether or not an installed valve was appropriate for determined possible changes and future projects within the plant [5]. A correction in one of the introduced formulas in the Displayed Control System was also carried out, where the flowrate of water steam sent to the flare was estimated as a function of the measured inlet temperature at the valve inlets, the measured pressure difference, and the measured aperture percentage of the involved regulation valves. The estimation of various equipment consumption as support information for possible savings was also carried out, as well as the update of a compressor's conversion chart after its revamping in order to check operating points.

The student also had the main task to deepen into the learning of the PSA process specifically, in order to decide an approach for the present project. A diverse number of possible software was considered, such as *Matlab*, *COMSOL Multiphysics®*, *Aspen Adsorption* and *gPROMS®*. With the aim of having the most flexibility as possible with dynamic tests, it was decided that *Aspen Adsorption* was the most appropriate tool for the planned approaches since the intrinsic model is already put into an interface arranged for process sequences that imply the manipulation of control valves.

The familiarization with the software took a considerable amount of time at the beginning, since the interface can be initially perceived as much less user-friendly than other more commonly used software tools from Aspen Technology. Once the user digs into the utilization and the manipulation of the software, the potential to simulate such a dynamically sensitive process as is a PSA system can be clearly noticed. In addition, there was a technical problem involving an outdated patch that unallowed the student to continue with simulation files that were saved and later executed again, for which *Aspen Technical Support* had to be contacted.

Apart from dynamic simulations, *Aspen Adsorption* also allows to execute cyclic steady state simulations, and apart from gas adsorption, other kinds of processes can be simulated such as ion-exchange processes and liquid adsorption processes, all of which are configured with distinct process blocks and streams that are arranged specifically for each approach.

In order to test the results provided by a simulation carried out with the Aspen Adsorption software, a paper by J. Xiao et al. was taken as a reference for a primary simulation of breakthrough curves. The feed composition is that of 60,4% Hydrogen, 28,1% methane and 11,5 carbon monoxide, under an adsorption pressure of 10 bar_a and an average feed flowrate of 6,8 L/min. A comparison of obtained results can be made from Figure 3. 1.

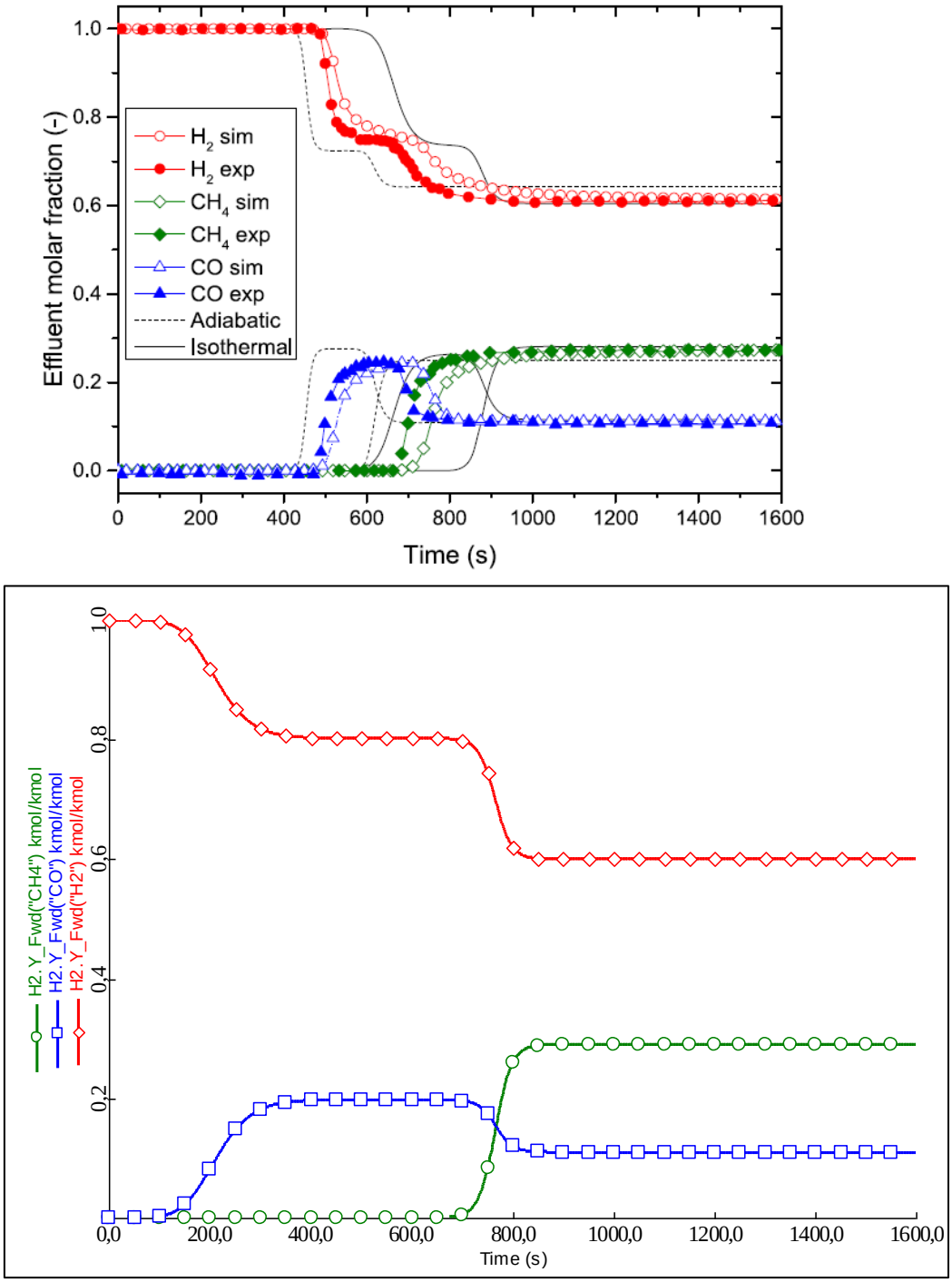

Figure 3. 1. Upper: Results from the research paper by Xiao et al., all rights reserved. Lower: Results obtained with an approximate simulation using *Aspen Adsorption*.

The results that were shown by Xiao et al. involved a single bed simulation with *COMSOL Multiphysics*®. The approximation made by the student with Aspen Adsorption was carried out considering an isothermal bed together with other simplifications such as a convection only material balance. The flowrate was approximated by means of a valve coefficient adjustment. The obtained results seemed to be more restrictive, as concentrations started de-stabilizing earlier, but the pattern of the molar fractions throughout time was similar to the one of reference. The valve coefficient could be further adjusted in order to resemble the breakthrough times to the reference.

After the software was tested and selected for the present project, the student deepened in the investigation and examination of the functioning sequence of the PDH plant's PSA unit in particular to understand and outline as realistically as possible the current operation sequence that the unit undergoes. Information about the sequence was extracted from the displayed control system with the help and support from the production department, and a summary for the operation of the unit made by *Emerson Process Management* was used as a support theoretical material to finish deducing the operating sequence. The sequence scheme of the PDH Plant's PSA unit drafted by Emerson© is shown in Appendix B.

4. METHODS AND APPROACH

The adsorbent bed model used for the different numerical simulations, as well as the different approaches used in order to comply with the project scope involving different configurations of a PSA system will be described herein.

4.1.Adsorbent bed model

The model for the adsorption bed used will be coequal for all of the subsequent simulations carried out throughout the project.

The bed is a vertical type, and it is composed by two different layers of adsorbent material as shown in Figure 4. 1.

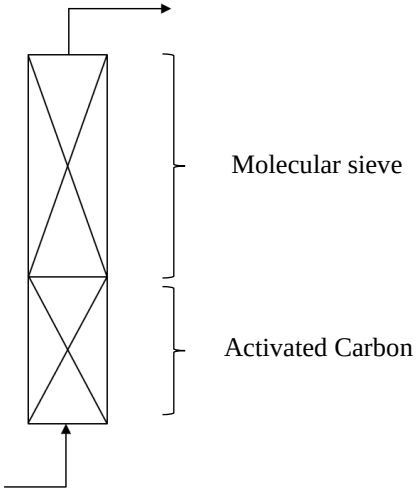

Figure 4. 1. Adsorbent bed loading diagram

The gas flux is assumed to be completely mixed in the radial direction, meaning that there are no radial gradients of concentration nor temperature. Thus, the simulation is carried out with a 1D component: spatial derivatives are evaluated in the axial flow direction only and the system is modelled as a plug flow with axial dispersion.

The spatial discretization method used is the Upwind Differencing Scheme of first order (UDS1). This method was chosen because it is a good all-round performer, being non-oscillatory and stable and the most efficient one in terms of simulation time whilst being fairly accurate, according to AspenTech® [6]. It also allows the accuracy to be later increased by increasing the number of nodes. In this case, the number of nodes is set to 20 for each adsorbent layer.

The specifications of both adsorbent layers present in a single bed are presented in Table 4. 1. [7]

Table 4. 1. Adsorbent bed specifications

	Layer 1 (Activated Carbon)	Layer 2 (Molecular Sieve 5A)
H_b (m)	2,96	4,39
W_t (m)	0,038	0,038
D_b (m)	1,50	1,50
ε_i (m^3 void / m^3 bed)	0,433	0,357
ε_p (m^3 void / m^3 bead)	0,61	0,65
ρ_s (kg/m^3)	850	1160
r_p (m)	$1{,}15 \cdot 10^{-3}$	$1{,}57 \cdot 10^{-3}$

Where H_b is the height of the adsorbent layer, W_t is the wall thickness, D_b is the internal diameter of the adsorbent layer, ε_i is the inter-particle voidage, ε_p is the intra-particle voidage, ρ_s is the bulk solid density of the adsorbent, and r_p is the adsorbent particle radius.

4.1.1. Material and momentum balance

For the material balance, convection with constant axial dispersion is assumed, meaning that the dispersion coefficient is considered constant for all of the components throughout the length of the bed, resulting in equation 4. 1 below.

$$-\varepsilon_i E_{zk} \frac{\partial^2 (C_k)}{\partial z^2} + \frac{\partial (v_g C_k)}{\partial z} + \varepsilon_B \frac{\partial C_k}{\partial t} + J_k = 0 \qquad (4.\ 1)$$

Axial dispersion | Convection | Gas phase accumulation | Flux rate to solid

Where E_{zk} is the axial dispersion coefficient of component *k*, C_k is the molar concentration of component *k*, v_g is the gas phase superficial velocity (also called Darcy's velocity), ε_b is the total bed voidage calculated from the combination of both the interparticle and the intraparticle voidages as in equation 4. 2, and J_k is the mass transfer rate of component *k* to the adsorbent, given by equation 4. 3.

$$\varepsilon_B = \varepsilon_i + (1 - \varepsilon_i)\varepsilon_p \qquad (4.\ 2)$$

$$J_k = -\rho_s \frac{\partial w_k}{\partial t} \qquad (4.\ 3)$$

The rate of adsorption follows a linear driving force solid-film model, which is later described during section 4.1.2. among the kinetic model.

The axial dispersion coefficient E_{zk} is calculated according to the following expression 4. 4. [8]

$$\frac{E_{zk}}{2v_g r_p} = \frac{20}{ReSc} + 0{,}5 \quad (4.\ 4)$$

Using the average calculated value for the superficial velocity, the axial dispersion coefficients result to be $6.13 \cdot 10^{-4}$ m^2/s and $5.64 \cdot 10^{-4}$ m^2/s for the Zeolite layer and the activated carbon layer, respectively.

For the momentum balance, it must be taken into consideration that the velocity as well as gas densities are linked to the pressure gradients among the bed, whether overall or locally. The Ergun equation has been preferred to describe the momentum balance (equation 4. 5), where the *Karman-Koenzy* equation (describing laminar flow) and the *Burke-Plummer* equation (describing turbulent flow) are combined [9]:

$$\frac{\partial P}{\partial z} = -\left(\frac{1{,}5 \cdot 10^{-3}(1-\varepsilon_i)^2}{(2r_p\psi)^2 {\varepsilon_i}^3}\mu v_g + 1{,}75 \cdot 10^{-5} M \rho_g \frac{(1-\varepsilon_i)}{2r_p \psi {\varepsilon_i}^3} v_g^2\right) \quad (4.\ 5)$$

Where ψ is the adsorbent shape factor, which has a value of 1 considering a spherical particle for the adsorbent, μ is the dynamic viscosity, M is the molecular weight and ρ_g is the gas phase molar density.

4.1.2. Kinetic model

The kinetic model corresponds to the formulation that will describe the transport of a species from the bulk gas domain to the solid domain (pore). The chosen approach is Lumped Resistance by Glueckauf [10], which is an overall form of the mass transfer rate model that determines how mass transfer due to adsorption takes place in the local gas and solid states. The hypothesis made is that all of the mass transfer resistance is lumped into a film that surrounds the adsorbent pellet and its loading is actually the driving force, contrary to the fluid film model, where the driving force was considered to remain in the fluid phase.

The model is selected in its linear form, where the mass transfer driving force for a component *k* is a linear function the solid phase loading (equation 4. 6).

$$\frac{\partial w_k}{\partial t} = MTC_{sk}(w_k^* - w_k) \quad (4.\ 6)$$

Where $\frac{\partial w_k}{\partial t}$ is the rate of adsorption, which was characterised as an accumulation term in the expression of the mass balance (see equations 4. 1 and 4. 3), MTC_{sk} is the solid-film mass transfer coefficient, and w_k^* is the loading of component *k* (defined as the component's molar concentration divided by the adsorbent density) at equilibrium with the actual gas phase concentration.

This lumped resistance approach implies that all the concentration gradients from the bulk gas to the solid are described with a single parameter, that is, the assumption that the overall mass transfer resistance is represented by a general factor.

Mass transfer coefficients are therefore considered constant, with the following experimental values given in Table 4. 2 [11].

Table 4. 2. Mass Transfer Coefficient values for each component and adsorbent.

Component	Mass Transfer Coefficient (s^{-1})	
	Activated carbon (Layer 1)	Zeolite 5A (Layer 2)
H_2	0,700	0,700
CH_4	0,195	0,147
CO	0,150	0,063

4.1.3. Isotherm

The isotherm model assumed for both layers is the extended Langmuir 3, which is a function of the solid phase temperature and partial pressure having the form given by equation 4. 7:

$$w_i = \frac{(IP_{1k} - IP_{2k}T_s)IP_{3k}e^{IP_{4k}/T_s}P_k}{1+\sum_{j=1}^{N}\left(IP_{3j}e^{IP_{4j}/T_s}P_j\right)} \quad (4.\ 7)$$

Where IP denotes a characterized isotherm parameter, and their values and units are presented in Table 4. 3 for the different gas phase components at each of the adsorbent layers.

Table 4. 3. Isotherm parameters for the Extended Langmuir 3 model.

Component	IP_1 (kmol/kg)	IP_2 (kmol/kg/K)	IP_3 (bar^{-1})	IP_4 (K)
	Activated carbon (Layer 1)			
H_2	0,01694	$2{,}10 \cdot 10^{-5}$	$0{,}625 \cdot 10^{-4}$	1229
CH_4	0,02386	$5{,}62 \cdot 10^{-5}$	$34{,}780 \cdot 10^{-4}$	1159
CO	0,03385	$9{,}07 \cdot 10^{-5}$	$2{,}311 \cdot 10^{-4}$	1751
	Zeolite 5A (Layer 2)			
H_2	0,00431	$1{,}06 \cdot 10^{-5}$	$25{,}15 \cdot 10^{-4}$	458
CH_4	0,00583	$1{,}19 \cdot 10^{-5}$	$6{,}05 \cdot 10^{-4}$	1731
CO	0,01184	$3{,}13 \cdot 10^{-5}$	$202{,}00 \cdot 10^{-4}$	763

4.1.4. Energy balance

In order to check temperature variations inside the system, the bed will be considered non-isothermal with gas phase conduction (the gas energy balance includes an axial thermal dispersion term), where the adsorbed components are considered to have constant heats of adsorption.

Regarding the wall energy balance, a rigorous heat transfer to the environment will be assumed (non-adiabatic). Assuming that the wall is sufficiently conductive and thin, the temperatures from both sides of it are established to be equal.

The gas phase energy balance is summed into the terms presented in equation 4. 8.

Axial thermal conduction | Convection | Gas phase accumulation | Compression | Gas-solid heat transfer | Gas-wall heat exchange

$$-\mathrm{k}_{gz}\varepsilon_i \frac{\partial^2 T_g}{\partial z^2} + C_{vg} v_g \rho_g \frac{\partial T_g}{\partial z} + \varepsilon_B C_{vg} \rho_g \frac{\partial T_g}{\partial t} + P \frac{\partial v_g}{\partial z} + \mathrm{HTC} a_p \left(\mathrm{T}_g - \mathrm{T}_s\right) + \frac{4H_w}{D_b}\left(\mathrm{T}_g - \mathrm{T}_0\right) = 0 \quad (4.\ 8)$$

Where k_g is the gas phase heat conductivity (considered constant), Cvg is the specific heat capacity of the gas at constant volume, HTC is the gas-solid heat transfer coefficient (assumed as 1 MW/m^2/K), a_p is the specific surface area of the adsorbent which is calculated according to equation 4. 9 below, H_w is the heat transfer coefficient between the gas and the wall (considered constant), and T_0 is the ambient temperature.

$$a_p = (1 - \varepsilon_i)\frac{3}{r_p} \quad (4.\ 9)$$

The solid phase energy balance is summed into equation 4. 10.

Accumulation | Heat of adsorbed phase | Heat of adsorption | Gas-solid heat transfer

$$\rho_s C_{ps} \frac{\partial T_s}{\partial t} + \rho_s \sum_{k=1}^{n} (C_{pak}\, \mathrm{w}_k) \frac{\partial T_s}{\partial t} + \rho_s \sum_{k=1}^{n} \left(\Delta H_k \frac{\partial w_k}{\partial t}\right) - \mathrm{HTC} a_p \left(\mathrm{T}_g - \mathrm{T}_s\right) = 0 \quad (4.\ 10)$$

Where C_{ps} is the adsorbent specific heat capacity, C_{pak} is the specific heat capacity of each gas phase component, and ΔH_k is the heat of adsorption for component k (considered constant).

Lastly, the wall energy balance is summed into equation 4. 11.

Axial thermal conduction | Heat accumulation within wall | Gas-wall heat exchange | Wall-environment heat exchange

$$-\mathrm{k}_w \frac{\partial^2 T_w}{\partial z^2} + \rho_w C_{pw} \frac{\partial T_w}{\partial t} - \mathrm{H}_w \frac{4D_b}{(D_b + W_t)^2 - {D_b}^2}\left(\mathrm{T}_g - \mathrm{T}_w\right) + \mathrm{H}_{amb} \frac{4(D_b + W_t)^2}{(D_b + W_t)^2 - {D_b}^2}\left(\mathrm{T}_w - \mathrm{T}_{amb}\right) = 0 \quad (4.\ 11)$$

Where k_w is the wall thermal conductivity, ρ_w is the wall density, C_{pw} is the wall specific heat capacity, and H_{amb} is the heat transfer coefficient between the wall and the ambient (constant).

The different parameters such as the component heats of adsorption and other thermal properties of both the bed and the vessel considered constant and used in the energy balance are summarised in Table 4. 4. and Table 4. 5. [12] [13] [14]

Table 4. 4. Heats of adsorption for each component and adsorbent layer.

Component	Heat of adsorption (MJ/kmol)	
	Activated carbon (Layer 1)	Zeolite 5A (Layer 2)
H_2	12,05	11,71
CH_4	17,95	22,59
CO	17,99	22,17

Table 4. 5. Constant parameters considered within the system's energy balance.

	Activated carbon (Layer 1)	Zeolite 5A (Layer 2)
C_{ps} (J/kg/K)	1046,5	920,9
C_{pw} (J/kg/K)	0,47	
H_{amb} (MW/m^2/K)	$3,7 \cdot 10^{-5}$	
H_w (MW/m^2/K)	$1 \cdot 10^{-4}$	
k_g (MW/m/K)	$4,52 \cdot 10^{-7}$	
K_w (MW/m/K)	$5,2 \cdot 10^{-5}$	
ρ_w (kg/m^3)	7861	

4.2. Simulation of the breakthrough curves

As a preliminary study, one single bed is simulated dynamically to obtain the breakthrough curves that later help estimating the maximum adsorption time for an hypothetical reached operation under cyclic steady state, depending on the established constraints.

The approach consists in feeding the initial mixture into the adsorber and plotting the time evolution of each of the component's molar fraction at the outlet of the adsorber bed. Both the adsorber and its outlet are assumed to be initially filled with pure hydrogen, so as to determine the time when the outlet starts to present the other components (implying the adsorbent is starting to saturate).

In Aspen Adsorption, it is not possible to directly connect active elements (such as valves and columns) without an intermediate dead space, that is, a component that acts as a conjunction to transfer the variables from one group of differential equations to another (node).

The flowsheet that represents one single adsorber column of the system was arranged using Aspen Adsorption as shown in Figure 4. 2.

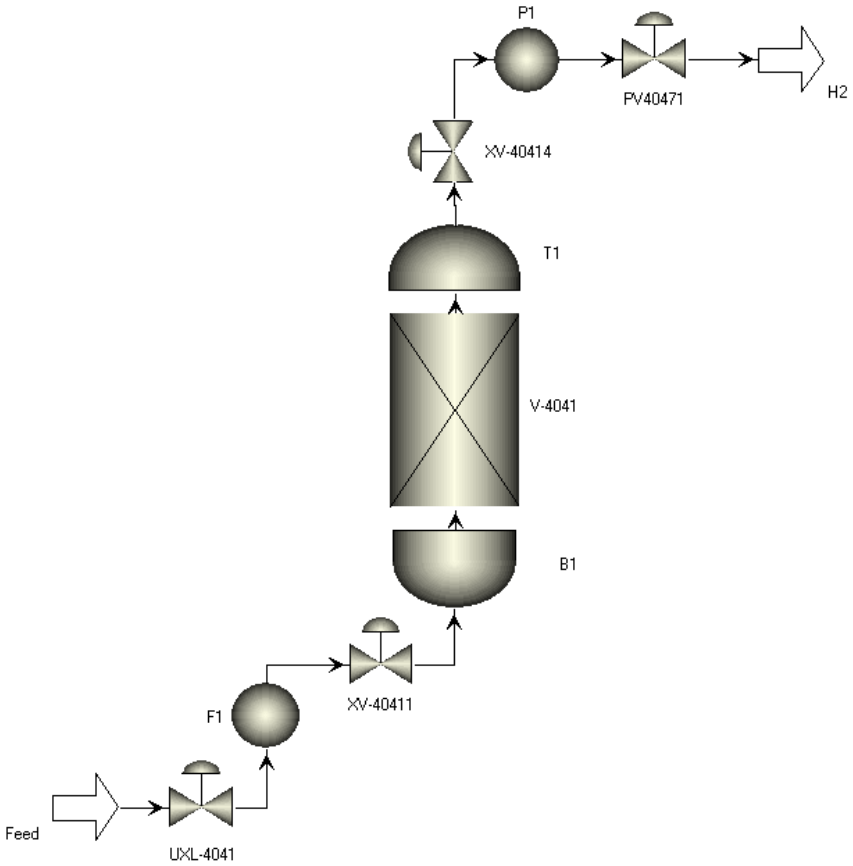

Figure 4. 2. Single adsorber flowsheet arranged in *Aspen Adsorption*.

The considered composition of the feeding stream (net gas) is fixed and equivalent to the one previously presented in Table 2. 2.

The components are defined in Aspen Properties®, where binary interaction is calculated using the Peng-Robinson approach, and they are later imported into Aspen Adsorption™.

In the feed block, it is convenient to leave the flowrate as a free variable if the pressure is to be fixed, or vice versa. In this approach, the pressure was fixed at 5,5 bar_g, and the flowrate was left as a free variable inside the feed block.

The product block is specified to be pure hydrogen, at a pressure of 5 bar_g and a temperature of 25ºC (according to the real plant data averages), and the flowrate is left as a free variable. The initial composition of the fluid that remains inside the bed is also set to be pure hydrogen.

The dead spaces are also set to be initially filled with pure hydrogen, but with the temperature and pressure analogue to those of the feed. Their volumes are primarily fixed to a value of 1 Nm^3.

If the column is working at the maximum pressure (that is, the feed pressure), it implies that most of the pressure drop should fall upon the outlet control valve (PV-40471). Based on the plant's PSA unit, the flowrate corresponding to pure hydrogen leaving the system is about _kmol/h. In order to distribute the desired flowrate along a pressure drop of 0,5 bar (5,5 bar_g at the inlet versus 5,0 bar_g at the outlet). The valve coefficient is therefore estimated to a value of _kmol/s/bar. In Aspen Adsorption, the characteristic of a valve doesn't vary in a quadratic form, but in a linear form to simplify the calculations. The interconnection valves XV-40411 and XV-40414 and the inlet valve UXL-4041 are simply left completely open.

An increased feed flowrate was also taken into consideration, with a reference value of _kg/h corresponding to a usual maximum flowrate of net gas entering the PSA, resulting in a product stream of _kg/h of hydrogen. For this case, the estimated valve coefficient is of _ kmol/s/bar. This peak feed flowrate (corresponding to _kmol/h) is tested because although it is not a direct input variable, it will be used as a reference feed flowrate to be achieved by the posterior simulations, as an increased flowrate constitutes a more restrictive case regarding purity as will be seen in section 5.1. Analysis of the Breakthrough curves.

Given that adsorption pressure is one of the key parametric studies for the case, valve coefficients were also estimated for different increased hypothetical feed pressures and for both product flowrates considered (_ and _ kmol/h). The pressure at the product outlet side is still considered to be at 5 bar_g, meaning, the pressure drop that will fall upon PV-40471 will be increased and it can be predicted that resulting valve coefficients will be much smaller than the ones at the base-case adsorption pressure of 5,5 bar_g.

A summary of the different valve coefficients estimated is shown in Table 4. 6.

Table 4. 6. Estimated valve coefficients for different adsorption pressures and product flowrates.

Adsorption pressure (bar_g)	Product valve coefficient (kmol/s/bar)	
	_ kmol/h H_2	_ kmol/h H_2
5,5	_	_
10	_	_
20	_	_
30	_	_

4.3. Base-case simulation of the 4-bed PSA system

To simulate the existing PSA system, a new flowsheet was created with four identical adsorbent beds to the one specified throughout section 4.1. The arrangement of the 4 bed-system is made based on the plant's existing unit with *Aspen Adsorption* as shown in Figure 4. 3 below.

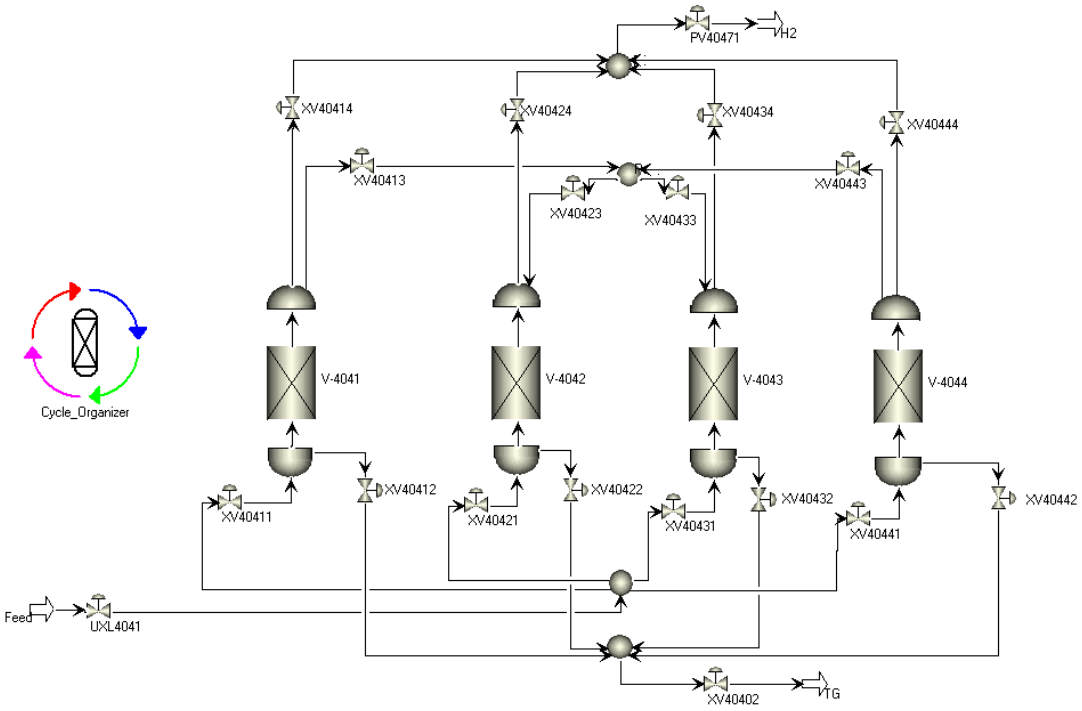

Figure 4. 3. Flowsheet arrangement for a four-bed PSA system in *Aspen Adsorption*.

The former simulation includes all the existing valves in the PSA unit, as well as the sequence arrangement for the flowsheet to mimic the cyclic operation of the process. In order to do so, a module called *Cycle Organizer* is used: this tool allows the definition of the step times and the interdependence in between them, as well as the control valve states at each step (manipulated variables). Once an entire cycle is defined within the simulation, the dynamic run will operate cyclically according to the defined constraints.

It is worth mentioning that the simulation is run by fixing pressure constraints, and thus flowrates as well as flow direction (with the latter concerning interconnection lines at the top of the columns) inside the system will fluctuate depending on pressure gradients and valve activity, as happens in the PSA unit process with the different cycle phases.

Taking into consideration the sequence description during section 2.1, a summary of the 4-bed sequence steps is summarized in Table 4. 7, complemented with the different valve activity changes defined within the cycle organizer, which are specified in Table 4. 8.

Table 4. 7. 4-Bed PSA sequence steps.

	Step nº											
Bed	1	2	3	4	5	6	7	8	9	10	11	12
V-4041	AD	AD	AD	PP	BD	BD	RP	I	P	P	P	AD
V-4042	P	P	AD	AD	AD	AD	PP	BD	BD	RP	I	P
V-4043	RP	I	P	P	P	AD	AD	AD	AD	PP	BD	BD
V-4044	PP	BD	BD	RP	I	P	P	P	AD	AD	AD	AD

*The shading indicates an adsorption overlap step

Table 4. 8. Valve operation specifications for each cycle step.

	Step nº											
Valve Tag	1	2	3	4	5	6	7	8	9	10	11	12
PV40471	2	2	2	2	2	2	2	2	2	2	2	2
UXL40401	1	1	1	1	1	1	1	1	1	1	1	1
XV40402	2	1	1	2	1	1	2	1	1	2	1	1
XV40411	1	1	1	0	0	0	0	0	0	0	0	1
XV40412	0	0	0	0	1	1	1	0	0	0	0	0
XV40413	0	0	0	1	0	0	2	0	0	0	0	0
XV40414	1	1	1	0	0	0	0	0	2	2	2	1
XV40421	0	0	1	1	1	1	0	0	0	0	0	0
XV40422	0	0	0	0	0	0	0	1	1	1	0	0
XV40423	0	0	0	0	0	0	1	0	0	2	0	0
XV40424	2	2	1	1	1	1	0	0	0	0	0	2
XV40431	0	0	0	0	0	1	1	1	1	0	0	0
XV40432	1	0	0	0	0	0	0	0	0	0	1	1
XV40433	2	0	0	0	0	0	0	0	0	1	0	0
XV40434	0	0	2	2	2	1	1	1	1	0	0	0
XV40441	0	0	0	0	0	0	0	0	1	1	1	1
XV40442	0	1	1	1	0	0	0	0	0	0	0	0
XV40443	1	0	0	2	0	0	0	0	0	0	0	0
XV40444	0	0	0	0	0	2	2	2	1	1	1	1

Connotation of each valve operation spec:
1: 100% Open
0: Closed
2: Control (use of Valve Coefficient)

As explained during the current PSA description, the four phase times are equal between them and at the same time divided in three different time frames that are regularly repeated, that is, $t_1 = t_4 = t_7 = t_{10} = 50$ s, $t_2 = t_5 = t_8 = t_{11} = 15$ s, and $t_3 = t_6 = t_9 = t_{12} = 5$ s. Therefore, steps are defined as time-driven and specified to be subsequent to each other.

Unlike the previous case of studying breakthrough curves with a single adsorbent bed, valve coefficients are not directly determined since one single CV ought to be defined for each valve but they actuate with different time frames and pressure drops throughout an entire cycle according to each different step.

The following expression 4. 12 is used to estimate initial values for the linear valve coefficients, as recommended by AspenTech. [15]

$$CV = \frac{100V}{RT\Delta t} ln\left(\frac{P_{high}^{start} - P_{low}^{start}}{P_{high}^{end} - P_{low}^{end}}\right) \quad (4.\ 12)$$

Where V is the bed to column interstitial volume plus gas volume in m^3 (calculated by following equation 4. 13, R is the universal gas constant in kJ/kmol/K, T is the gas temperature, Δt is the step time in seconds, and P is the pressure in bar_a, with the superscript indicating the start or end of the step, and the subscript indicating the high or the low pressure side of the valve.

$$V = \left(\varepsilon_i + \varepsilon_p(1 - \varepsilon_i)\right) H_b \left(\frac{D_b}{2}\right)^2 \pi \quad (4.\ 13)$$

The resulting interstitial volume is of 10 m^3, with 4 m^3 and 6 m^3 corresponding to the active carbon and zeolite layers, respectively.

In the case of XV-404X3 valves, these have a control action during Receive Purge steps (50 seconds), With a high starting and ending pressures of 1,5 bar_g and low starting and ending pressures of 0,3 and 1,4 bar_g, respectively.

Regarding product valves (XV-404X4), they have a control action during the re-pressurization steps (70s), With high starting and ending pressures of 5,5 bar_g and low starting and ending pressures of 1,5 and 5,4 bar_g, respectively.

For the tail gas, its valve is being controlled during Blowdown steps (20 s), where the high starting and ending pressures are 1,5 and 0,4 barg respectively, and low starting and ending pressures are approximated to 0,5 and 0,3 barg, respectively.

Regarding the product valve, it is simply adjusted to a CV that allows an average reference flowrate of _ kmol/h.

The estimated valve coefficients (specification "2" above in Table 4. 8) were later adjusted in order to comply with restrictions such as the product purity specification, being summarised in Table 4. 9.

Table 4. 9. Valve coefficient specifications for the four-bed PSA system at 5,5 bar_g.

	Valve Tag			
	PV40471	XV40402	XV404X3	XV404X4
CV (kmol/s/bar)	0,12	$4{,}68 \cdot 10^{-2}$	0,02	0,05

4.4. Simulation of a 4-bed PSA system with increased adsorption pressure

In the simulated test of a 4-bed system with an increased adsorption pressure, the sequence stays as specified in section 4.3 regarding steps and subsequent valve activation patterns, but the step times are slightly increased as follows: $t_1 = t_4 = t_7 = t_{10} = 80$ s, $t_2 = t_5 = t_8 = t_{11} = 25$ s, and $t_3 = t_6 = t_9 = t_{12} = 10$ s.

Taking this into consideration, together with the approach of fixing the tail gas pressure at the same value as the base-case to have broader pressure oscillations and the outlet of the product valve PV-40471 at 5 bar_g, the valve coefficients are adjusted and specified within the simulation to the values shown in Table 4. 10.

Table 4. 10. Valve coefficient specifications for a four-bed PSA system at 30 bar_g.

	Valve Tag			
	PV40471	XV40402	XV404X3	XV404X4
CV (kmol/s/bar)	0,004	$5{,}32 \cdot 10^{-2}$	0,002	$1{,}86 \cdot 10^{-2}$

Although higher hydrogen recoveries can be achieved by increasing the feed pressure, it was also considered to slightly modify the 4-bed system with the aim of having a zero idle time and increase the pressure equalization steps (provide/receive purge) from 1 pair to 2 pairs per bed sequence. This can be done by dividing the manifold that XV-404X3 valves constitute into two different manifolds, one of which is communicated with the hydrogen product line to comply with the re-pressurization steps. [16]

In the following Figure 4. 4, XV-404X5 valves constitute the first pressure equalization manifold (on/off valves), which is also communicated to the hydrogen product manifold via the XV-40404 regulation valve, and XV-404X6 constitute the second pressure equalization manifold (on/off valves).

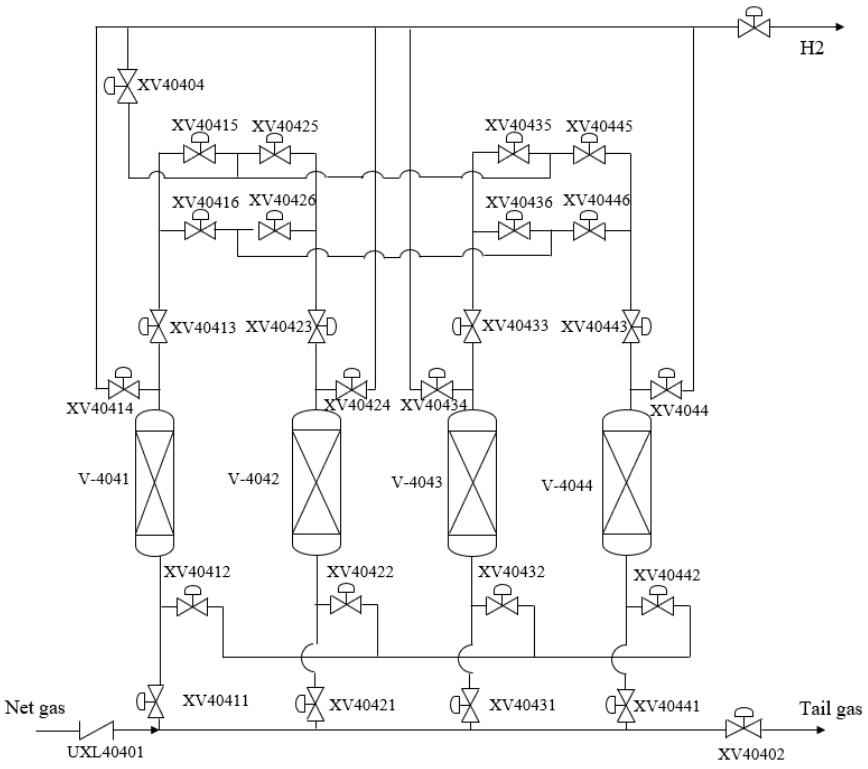

Figure 4. 4. Draft of a four-bed PSA system with two different pressure equalization manifolds.

The sequence is scheduled as shown in Figure 4. 5, the steps of which are explained below.

Bed	Phase nº											
	1			2			3			4		
	Step nº											
	1	2	3	4	5	6	7	8	9	10	11	12
V-4041	AD			PP1	PT	PP2	BD	PR	RP1	RP2	P1	P2
		P1	P2									
V-4042	BD	PR	RP1	RP2	P1	P2	AD			PP1	PT	PP2
							P1	P2				
V-4043	PP1	PT	PP2	BD	PR	RP1	RP2	P1	P2	AD		
										P1	P2	
V-4044	RP2	P1	P2	AD			PP1	PT	PP2	BD	PR	RP1
				P1	P2							

Figure 4. 5. Sequence scheme of a four-bed PSA system with two pressure equalisation steps.

During step 1, bed 1 undergoes the adsorption step, whilst bed 2 is in blowdown. Bed 3 is in its first provide purge step, as it is communicating with bed 4 via the first manifold, which is already in its second receive purge step.

In step 2, while bed 1 is still undergoing the adsorption step, a slipstream is extracted via the first manifold by opening the intercommunication valve to repressurize bed 4. Bed 2 is in its purge step, which means that it is now having a stream that purges counter-currently via the second manifold coming from bed 3's top side, which is purging co-currently.

During step 3, beds 1 and 4 are undergoing the same process as in the previous step. Bed 2 now receives purge from bed 3 (which is now going through its second provide purge step) via the second manifold, by also closing and opening their tail gas valves, respectively.

In step 4, which starts the second phase of the sequence, bed 1 has finished the adsorption phase and enters its first provide purge step to bed 2, which receives the purge as it is its second receive purge step. Bed 3 goes through a blowdown independently and bed 4 starts its adsorption phase.

During step 5, bed 1 purges co-currently as bed 3 receives it counter-currently. Bed 2 now enters the re-pressurization step, by having a split stream of hydrogen coming from bed 4 which is still in the adsorption step.

In step 6, beds 2 and 4 are undergoing the same process as in the previous step. Bed 1 now enters its second provide purge step, which is received by bed 3 as its first receive purge step.

Throughout step 7, bed 1 goes through a blowdown independently, whilst bed 2 starts its adsorption phase. Bed 3 receives its second purge, which comes from bed 4 with its first provide purge step after its adsorption phase.

During step 8: Bed 1 receives pressure counter-currently, provided by the co-current purge from bed 4. Bed 2 now provides a slipstream of hydrogen to bed 3 while it still undergoes the adsorption step to start re-pressurizing bed 3.

In step 9, beds 2 and 3 are undergoing the same phase as in the previous step, whilst bed 1 is receiving its first purge from bed 4, which undergoes its second provide purge step.

Through step 10, bed 1 receives its second purge from bed 2, which now has finished its adsorption phase. Bed 3 starts its adsorption phase, whilst bed 4 undergoes a blowdown by itself.

In step 11, bed 1 starts re-pressurizing by means of a split stream of hydrogen from the adsorption taking place in bed 3. Bed 2 now purges co-currently as bed 4 receives its pressure and purges counter-currently.

Finally, during step 12, bed 1 enters its final re-pressurization step with the hydrogen coming from bed 3 in adsorption, and bed 2 undergoes its second provide purge step which is received by bed 4 for the first time. Once this phase finishes, the cycle starts all over again back to step 1 and so it repeats the sequence pattern cyclically.

Table 4. 11. summarises all of the valve activity changes throughout the sequence previously described.

Table 4. 11. Valve specifications in a four-bed and two pressure equalisation sequence.

	Step nº											
Valve Tag	1	2	3	4	5	6	7	8	9	10	11	12
PV40471	2	2	2	2	2	2	2	2	2	2	2	2
UXL40401	1	1	1	1	1	1	1	1	1	1	1	1
XV40402	2	2	2	2	2	2	2	2	2	2	2	2
XV40404	0	2	2	0	2	2	0	2	2	0	2	2
XV40411	1	1	1	0	0	0	0	0	0	0	0	0
XV40412	0	0	0	0	0	1	1	1	0	0	0	0
XV40413	0	0	0	2	2	2	0	1	1	1	1	1
XV40414	1	1	1	0	0	0	0	0	0	0	0	0
XV40415	0	0	0	1	0	0	0	0	0	1	1	1
XV40416	0	0	0	0	1	1	0	1	1	0	0	0
XV40421	0	0	0	0	0	0	1	1	1	0	0	0
XV40422	1	1	0	0	0	0	0	0	0	0	0	1
XV40423	0	1	1	1	1	1	0	0	0	2	2	2
XV40424	0	0	0	0	0	0	1	1	1	0	0	0
XV40425	0	0	0	1	1	1	0	0	0	1	0	0
XV40426	0	1	1	0	0	0	0	0	0	0	1	1
XV40431	0	0	0	0	0	0	0	0	0	1	1	1
XV40432	0	0	1	1	1	0	0	0	0	0	0	0
XV40433	2	2	2	0	1	1	1	1	1	0	0	0
XV40434	0	0	0	0	0	0	0	0	0	1	1	1
XV40435	1	0	0	0	0	0	1	1	1	0	0	0
XV40436	0	1	1	0	1	1	0	0	0	0	0	0
XV40441	0	0	0	1	1	1	0	0	0	0	0	0
XV40442	0	0	0	0	0	0	0	0	1	1	1	0
XV40443	1	1	1	0	0	0	2	2	2	0	1	1
XV40444	0	0	0	1	1	1	0	0	0	0	0	0
XV40445	1	1	1	0	0	0	1	0	0	0	0	0
XV40446	0	0	0	0	0	0	0	1	1	0	1	1

Connotation of each valve operation spec:
1: 100% Open
0: Closed
2: Control (use of Valve Coefficient)

The step times for this approach are also based on the referenced patent, being of $t_1 = t_4 = t_7 = t_{10} = 40$ s, $t_2 = t_5 = t_8 = t_{11} = 85$ s, and $t_3 = t_6 = t_9 = t_{12} = 25$ s. It is worth noting that in this sequence the adsorption step is elapsed with respect to the previous one, starting in step 1 for the first bed instead of in step 12. It is on account of this lapse that for this approach, the sequence doesn't start off with the largest time frame step.

Table 4. 12. shows the valve coefficients adjusted and used for this simulation to adjust to a feed flowrate reference value close to _ kmol/h and to reach a cyclic steady state product composition under specification.

Table 4. 12. Adjusted valve coefficients for a four-bed PSA system with two pressure equalisation steps.

	Valve Tag				
	PV40471	XV40402	XV404X3	XV404X4	XV40404
CV (kmol/s/bar)	$4{,}3 \cdot 10^{-3}$	0,1	$6 \cdot 10^{-3}$	$2 \cdot 10^{-3}$	0,015

4.5. Simulation of a 6-bed PSA system at the original adsorption pressure

To further increase a PSA system's recovery, there ought to be a higher number of pressure equalization (provide/receive purge) steps. With a four-bed system, there can be two different pressure equalization pair steps per bed cycle (two for decreasing pressure and two for increasing pressure), but with a 6-bed system, there can be four different pressure equalization pair steps per bed cycle whilst also having a zero idle time.

The simulation is based upon US patent no. 8,491,704 B2, which introduces three different manifolds to intercommunicate the top side of the six different beds, one of which can be connected to the hydrogen product line by means of an extra valve, as was in the previous case [17]. The arrangement of the system is shown in Figure 4. 6.

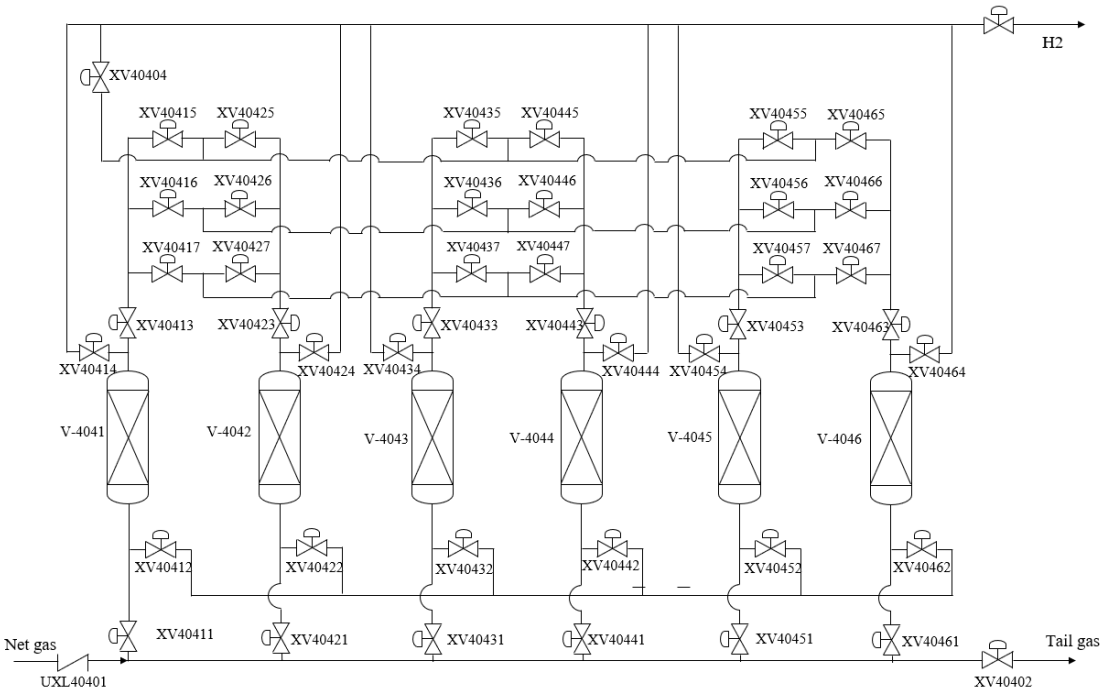

Figure 4. 6. Flowsheet of a six-bed PSA system.

XV-404X5, XV-404X6 and XV-404X7 valves are on/off valves, whilst the XV-40404 valve is a regulated control valve.

The step sequence is scheduled as schematized in Figure 4. 7. and explained hereunder.

Bed	Phase n°																	
	1			2			3			4			5			6		
	Step n°																	
	1	2	3	4	5	6	7	8	9	10	11	12	13	14	15	16	17	18
V-4041	AD			PP1	PP2		PP3	PT	PP4	BD	PR	RP4	RP3	RP2		RP1	P1	P2
	P1	P2																
V-4042	RP1	P1	P2	AD			PP1	PP2		PP3	PT	PP4	BD	PR	RP4	RP3	RP2	
				P1	P2													
V-4043	RP3	RP2		RP1	P1	P2	AD			PP1	PP2		PP3	PT	PP4	BD	PR	RP4
							P1	P2										
V-4044	BD	PR	RP4	RP3	RP2		RP1	P1	P2	AD			PP1	PP2		PP3	PT	PP4
										P1	P2							
V-4045	PP3	PT	PP4	BD	PR	RP4	RP3	RP2		RP1	P1	P2	AD			PP1	PP2	
													P1	P2				
V-4046	PP1	PP2		PP3	PT	PP4	BD	PR	RP4	RP3	RP2		RP1	P1	P2	AD		
																P1	P2	

Figure 4. 7. Sequence scheme of a six-bed PSA system.

During the Adsorption step (AD), the feed and product valves of the bed are completely opened (XV-404X1 and XV-404X4, respectively). In the last two time frames of this step, a slipstream of hydrogen is provided to the bed that has to re-pressurize via the regulation of the XV-40404 valve.

The provide purge steps (PPX) work as in the previous cases: the intercommunication valve regulates the flowrate (XV-404X3), and a specific on/off valve opens accordingly to the manifold that must be used to connect to a particular bed that undergoes a receive purge step. The fourth provide purge step is different in the sense that it can also be assimilated to a first blowdown step, as it involves also opening the tail gas valve (XV-404X2).

The purge top (PT) step is a co-current de-pressurization step, which is similar to a provide purge step, with the difference that the bed that receives it is not on a receive-purge step to increase its pressure, but on a counter-current depressurization step by opening its tail gas valve (XV-404X2).

The blowdown step (BD) involves opening only the tail gas valve, further depressurizing the bed by equalizing its pressure to the lowest available.

The purge step (PR) is a counter-current depressurization step, where the purge flow is provided by a bed on its purge top (co-current depressurization) step.

The different receive purge steps (RPX) consist of receiving the flowrate from a bed undergoing a provide purge step by completely opening the corresponding intercommunication valves.

The re-pressurization steps (PX) entail completely opening the intercommunication valves at the first manifold of the top side of the bed (XV-404X3 and XV-404X5), however this time it is communicated to the product line of hydrogen by regulating the XV-40404 valve.

A summary of the valve activity specifications throughout the different sequence steps is presented in Table 4. 13.

Table 4. 13. Valve activity specifications for a six-bed PSA system.

Valve Tag	Step nº																	
	1	2	3	4	5	6	7	8	9	10	11	12	13	14	15	16	17	18
PV40471	2	2	2	2	2	2	2	2	2	2	2	2	2	2	2	2	2	2
UXL40401	1	1	1	1	1	1	1	1	1	1	1	1	1	1	1	1	1	1
XV40402	2	2	2	2	2	2	2	2	2	2	2	2	2	2	2	2	2	2
XV40404	0	2	2	0	2	2	0	2	2	0	2	2	0	2	2	0	2	2
XV40411	1	1	1	0	0	0	0	0	0	0	0	0	0	0	0	0	0	0
XV40412	0	0	0	0	0	0	0	0	1	1	1	0	0	0	0	0	0	0
XV40413	0	0	0	2	2	2	2	2	2	0	1	1	1	1	1	1	1	1
XV40414	1	1	1	0	0	0	0	0	0	0	0	0	0	0	0	0	0	0
XV40415	0	0	0	1	0	0	0	0	0	0	0	0	0	0	0	1	1	1
XV40416	0	0	0	0	1	1	1	0	0	0	0	0	1	1	1	0	0	0
XV40417	0	0	0	0	0	0	0	1	1	0	1	1	0	0	0	0	0	0
XV40421	0	0	0	1	1	1	0	0	0	0	0	0	0	0	0	0	0	0
XV40422	0	0	0	0	0	0	0	0	0	0	0	1	1	1	0	0	0	0
XV40423	1	1	1	0	0	0	2	2	2	2	2	2	0	1	1	1	1	1
XV40424	0	0	0	1	1	1	0	0	0	0	0	0	0	0	0	0	0	0
XV40425	1	1	1	0	0	0	1	0	0	0	0	0	0	0	0	0	0	0
XV40426	0	0	0	0	0	0	0	1	1	1	0	0	0	0	0	1	1	1
XV40427	0	0	0	0	0	0	0	0	0	0	1	1	0	1	1	0	0	0
XV40431	0	0	0	0	0	0	1	1	1	0	0	0	0	0	0	0	0	0
XV40432	0	0	0	0	0	0	0	0	0	0	0	0	0	0	1	1	1	0
XV40433	1	1	1	1	1	1	0	0	0	2	2	2	2	2	2	0	1	1
XV40434	0	0	0	0	0	0	1	1	1	0	0	0	0	0	0	0	0	0
XV40435	0	0	0	1	1	1	0	0	0	1	0	0	0	0	0	0	0	0
XV40436	1	1	1	0	0	0	0	0	0	0	1	1	1	0	0	0	0	0
XV40437	0	0	0	0	0	0	0	0	0	0	0	0	0	1	1	0	1	1
XV40441	0	0	0	0	0	0	0	0	0	1	1	1	0	0	0	0	0	0
XV40442	1	1	0	0	0	0	0	0	0	0	0	0	0	0	0	0	0	1
XV40443	0	1	1	1	1	1	1	1	1	0	0	0	2	2	2	2	2	2
XV40444	0	0	0	0	0	0	0	0	0	1	1	1	0	0	0	0	0	0
XV40445	0	0	0	0	0	0	1	1	1	0	0	0	1	0	0	0	0	0
XV40446	0	0	0	1	1	1	0	0	0	0	0	0	0	1	1	1	0	0
XV40447	0	1	1	0	0	0	0	0	0	0	0	0	0	0	0	0	1	1
XV40451	0	0	0	0	0	0	0	0	0	0	0	0	1	1	1	0	0	0
XV40452	0	0	1	1	1	0	0	0	0	0	0	0	0	0	0	0	0	0
XV40453	2	2	2	0	1	1	1	1	1	1	1	1	0	0	0	2	2	2
XV40454	0	0	0	0	0	0	0	0	0	0	0	0	1	1	1	0	0	0
XV40455	0	0	0	0	0	0	0	0	0	1	1	1	0	0	0	1	0	0
XV40456	1	0	0	0	0	0	1	1	1	0	0	0	0	0	0	0	1	1
XV40457	0	1	1	0	1	1	0	0	0	0	0	0	0	0	0	0	0	0
XV40461	0	0	0	0	0	0	0	0	0	0	0	0	0	0	0	1	1	1
XV40462	0	0	0	0	0	1	1	1	0	0	0	0	0	0	0	0	0	0
XV40463	2	2	2	2	2	2	0	1	1	1	1	1	1	1	1	0	0	0
XV40464	0	0	0	0	0	0	0	0	0	0	0	0	0	0	0	1	1	1
XV40465	1	0	0	0	0	0	0	0	0	0	0	0	1	1	1	0	0	0
XV40466	0	1	1	1	0	0	0	0	0	1	1	1	0	0	0	0	0	0
XV40467	0	0	0	0	1	1	0	1	1	0	0	0	0	0	0	0	0	0

For this approach, the step times are adjusted as follows: $t_1 = t_4 = t_7 = t_{10} = t_{13} = t_{16} = 10$ s, $t_2 = t_5 = t_8 = t_{11} = t_{14} = t_{17} = 25$ s, and $t_3 = t_6 = t_9 = t_{12} = t_{15} = t_{18} = 5$ s.

Table 4. 14. shows the adjusted valve coefficients for a feed flowrate close to _ kmol/h whilst achieving a cyclic steady state where the product molar composition is under specification.

Table 4. 14. Adjusted valve coefficients for a six-bed PSA system at 5,5 bar_g.

	Valve Tag				
	PV40471	XV40402	XV404X3	XV404X4	XV40404
CV (kmol/s/bar)	0,153	$4 \cdot 10^{-2}$	$4 \cdot 10^{-2}$	$1{,}2 \cdot 10^{-1}$	$4 \cdot 10^{-2}$

4.6. Simulation of a 6-bed PSA system with an increased adsorption pressure

The four equalization steps that can be achieved with a 6-bed system are most likely to not be fully taken advantage of with a relatively low adsorption pressure equal to that of the original net gas feeding pressure, 5,5 bar_g. With the aim of maximizing hydrogen production, a higher adsorption pressure can be introduced into the 6-bed system, that is, increasing the pressure at the feed.

When the pressure ratio between the feed (adsorption pressure) and the tail gas is higher than 10, a system of 6 beds is already suggested according to UOP also for small capacity units (<5000 Nm^3/h) due to having the possibility of increasing the number of pressure equalization steps within the sequence altogether with having a zero idle time.

The flowsheet arrangement as well as the sequence steps are the same as in section 4.5, but valve coefficients are readjusted to the values presented in Table 4. 15.

Table 4. 15. Adjusted valve coefficients for a six-bed PSA system at 30 bar_g.

	Valve Tag				
	PV40471	XV40402	XV404X3	XV404X4	XV40404
CV (kmol/s/bar)	0,0047	0,1	$2 \cdot 10^{-3}$	$6 \cdot 10^{-3}$	$2 \cdot 10^{-2}$

Step times are also readjusted as follows based on the referenced patent: $t_1 = t_4 = t_7 = t_{10} = t_{13} = t_{16} = 25$ s, $t_2 = t_5 = t_8 = t_{11} = t_{14} = t_{17} = 65$ s, and $t_3 = t_6 = t_9 = t_{12} = t_{15} = t_{18} = 15$ s.

5. RESULTS AND DISCUSSION

With the results obtained from the different simulations approached as described throughout section 4, these are discussed herein with the objective of deciding the posterior revamping approach and assess its economic cost and obtainable profit in the long-term.

5.1. Analysis of the Breakthrough curves

Firstly, the breakthrough curves are simulated according to the approach described in section 4.2.

Breakthrough curves are simulated at four different pressure values in the range between 5,5 bar_g and 30 bar_g and for a flowrate of about _ kmol/h, which corresponds to the average value of hydrogen product. The effect of pressure in the different breakthrough curves for each component is shown from Figure 5. 1 to Figure 5. 3.

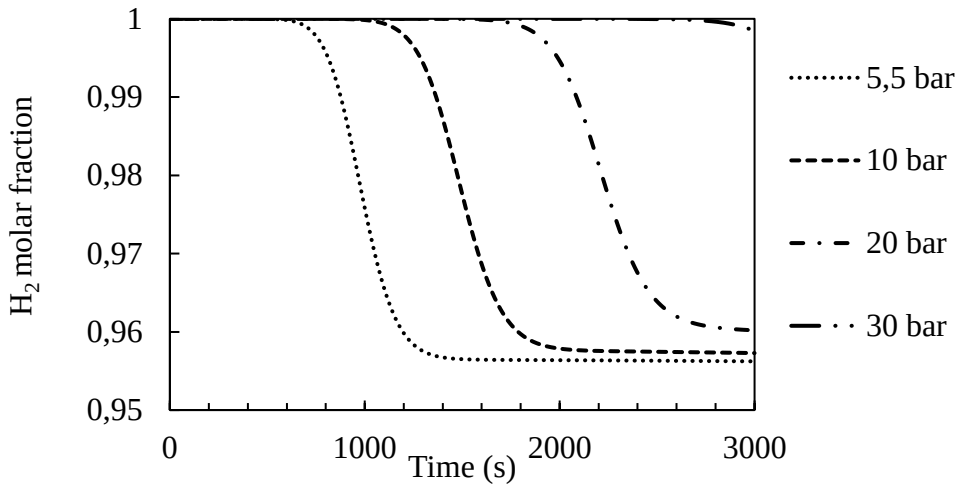

Figure 5. 1. Breakthrough curves for hydrogen at different adsorption pressures with a product flowrate equivalent to _ kmol/h.

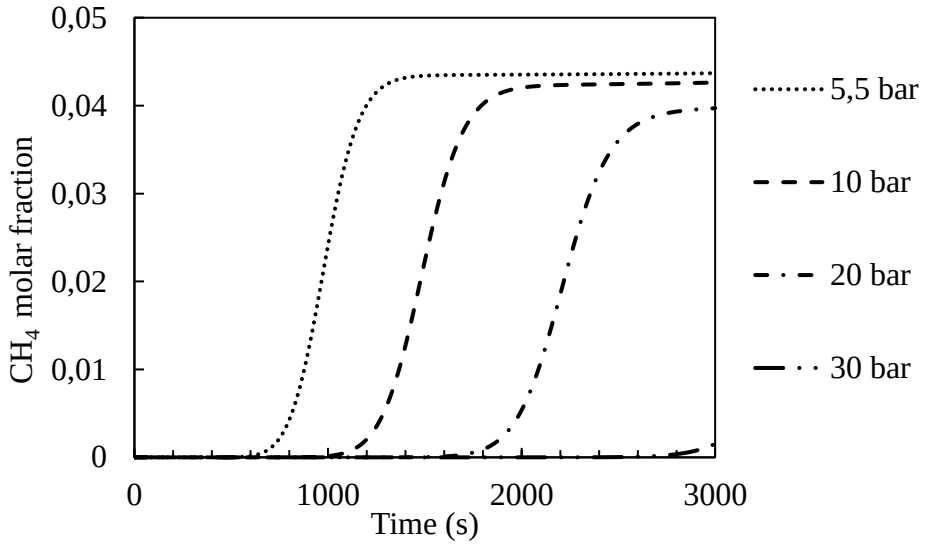

Figure 5. 2. Breakthrough curves for methane at different adsorption pressures with a product flowrate equivalent to _ kmol/h.

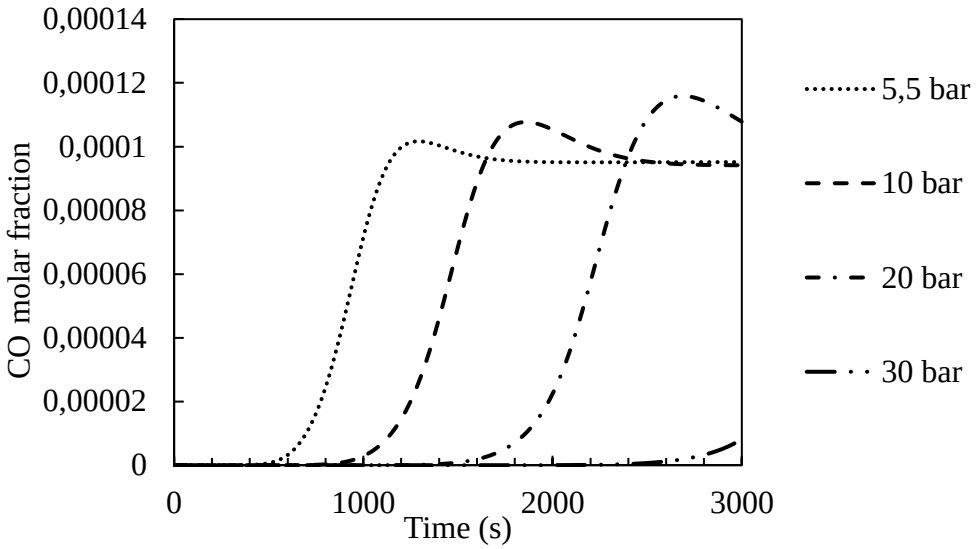

Figure 5. 3. Breakthrough curves for carbon monoxide at different adsorption pressures with a product flowrate equivalent to _ kmol/h.

It can be noted that as operating pressure increases, the product flow starts to have a decreased hydrogen composition much later than with lower operating pressures. Likewise, the impurities start to gain notoriety at the product much later with increased adsorption pressures.

Although it is known that increasing adsorption pressure yields for higher hydrogen recoveries, and thus the hydrogen availability is increased in time, it should also be taken into consideration that the experiments in which the isotherm models are based were carried out at pressures not higher than 10 bar_g, and thus a certain accuracy cannot be assured. Even so, the tendency of breakthrough curves to be slowed down with increasing pressure is correct and supported by adsorption theory.

In the case of an adsorption pressure of 5,5 bar_g, hydrogen purity starts to decay at lower values than _% molar purity from second 74 forward. In turn, carbon monoxide has a _ppm molar concentration at the product flow up until second 483 of the simulation, so as long as the adsorption step is cut out before 74 seconds have passed, the product stream ought to be inside specification.

For an increased adsorption pressure up to 30 bar_g, hydrogen purity decays from an even further simulation time value, at 357 seconds. Regarding carbon monoxide, it reaches a _ppm molar composition at the product at time 2444, so in principle, as long the adsorption phase time is inside the frame of 357 seconds, the product outlet at an increased adsorption pressure complies with the requirements.

The peak feed flowrate that is fed to the PSA system reaches a value around _ kg/h, which corresponds to a more restrictive case since the flowrate of hydrogen would increase, meaning that the adsorbent would saturate earlier and thus the adsorption phase time can be considered to be shorter. This feed flowrate corresponds to a hydrogen product of _ kg/h (_ kmol/h), and the breakthrough curves were as well simulated for an adsorption pressure range from 5,5 bar_g to 30 bar_g as shown from Figure 5. 4 to Figure 5. 6.

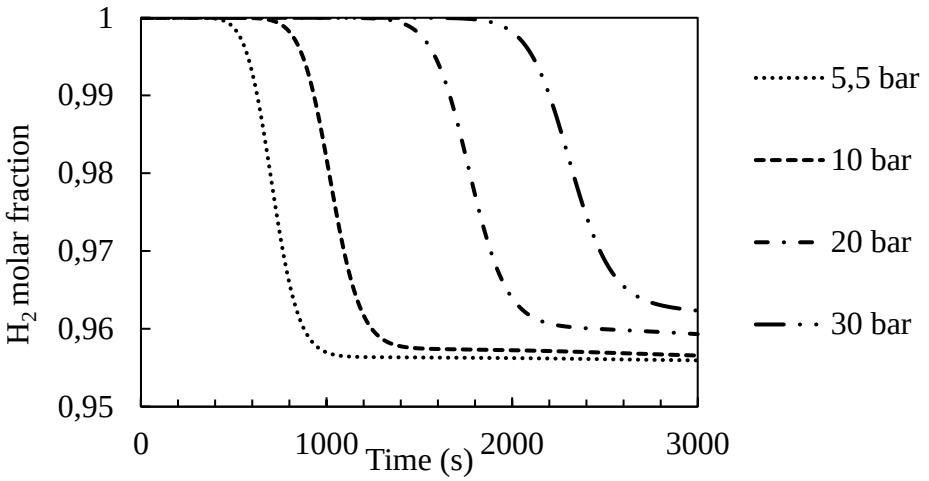

Figure 5. 4. Breakthrough curves for hydrogen at different adsorption pressures with a product flowrate equivalent to _ kmol/h.

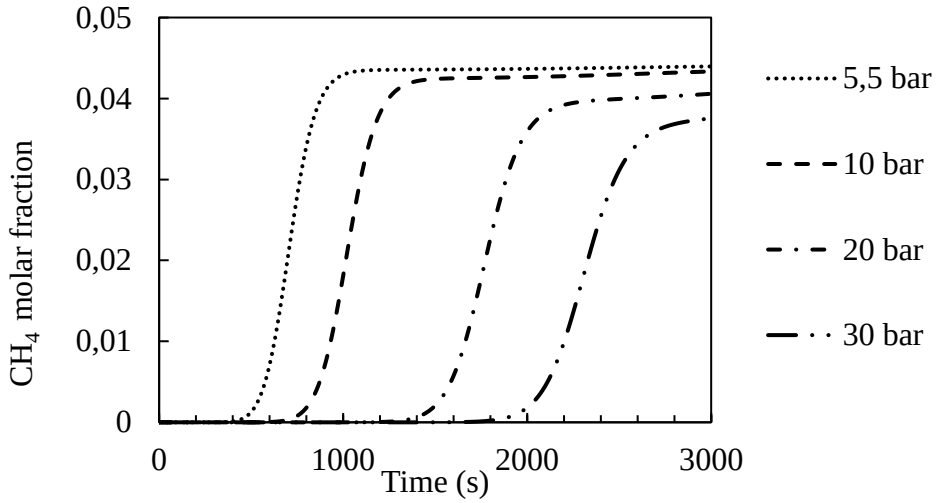

Figure 5. 5. Breakthrough curves for methane at different adsorption pressures with a product flowrate equivalent to _ kmol/h.

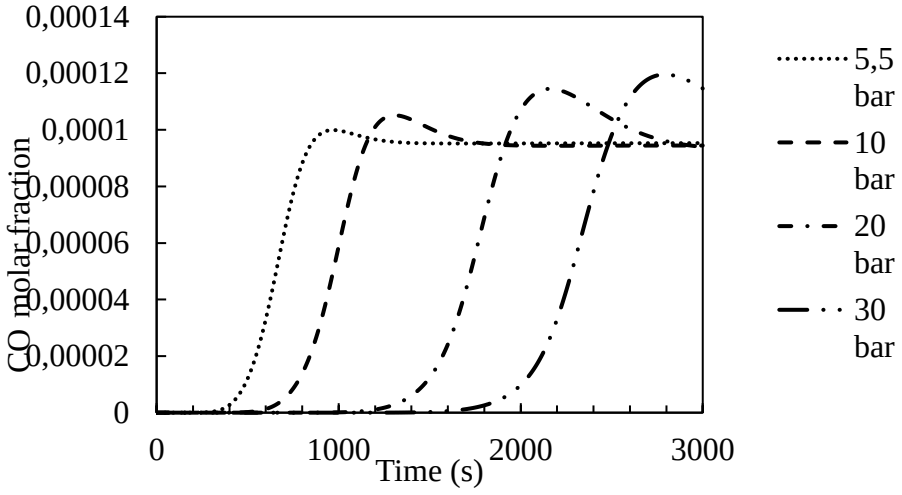

Figure 5. 6. Breakthrough curves for carbon monoxide at different adsorption pressures with a product flowrate equivalent to _ kmol/h.

For the lowest adsorption pressure value considered (5,5 bar_g), hydrogen purity decays to values lower than a _% molar from time stamp = 50 s and beyond. As for carbon monoxide, it shows values higher than a _ppm molar composition from second 320.

At higher adsorption pressures, specifically for the highest value of 30 bar_g, adsorption phase time is not as restrictive since hydrogen purity starts decaying from _% molar at second 235. As for carbon monoxide, it shows molar composition values out of specification at simulation time equal to 1587.

Although the tendency is similar at both reference flowrates, the fact that the actual PSA feed flowrate can rise up to _kg/h and beyond means that it needs to be taken into consideration for the adsorption time, as it should be shortened if the purity needs to be maintained as high as possible. Once purity decays, the same hydrogen flow is also used to regenerate the different adsorbent beds during pressure equalization and re-pressurization steps, subsequently limiting purity for further cycles.

With the aim of seeing the tendency of the front of impurities at the gas phase passing through the adsorbent bed, breakthrough curves were simulated along the different bed nodes throughout the 1D component that represents the length of the bed, as shown from Figure 5. 7 to Figure 5. 9. Node 0 corresponds to the inlet of the vessel (bottom side) and node 40 to the outlet of the vessel (top side). These were simulated at a reference product flowrate of _ kmol/h and 5,5 bar_g of adsorption pressure.

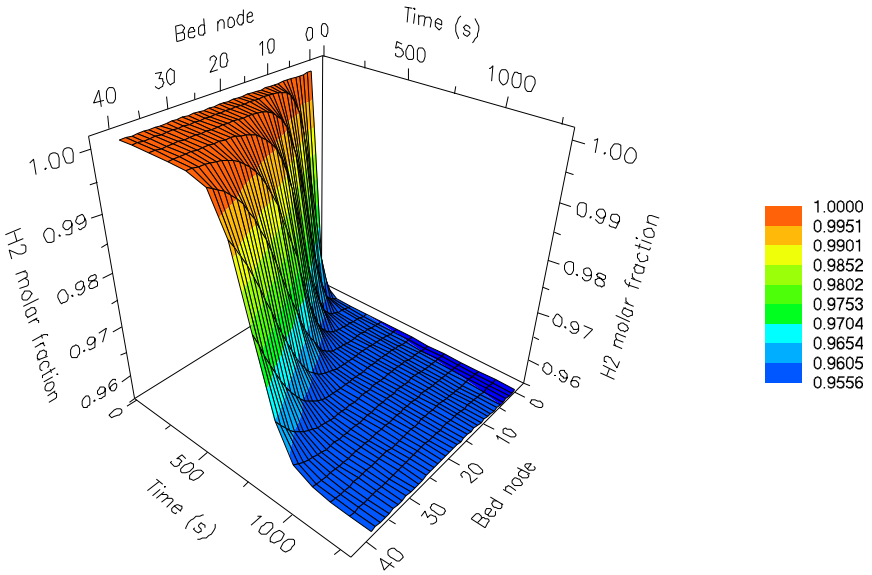

Figure 5. 7. Adsorption breakthrough curves for hydrogen along the bed calculation nodes.

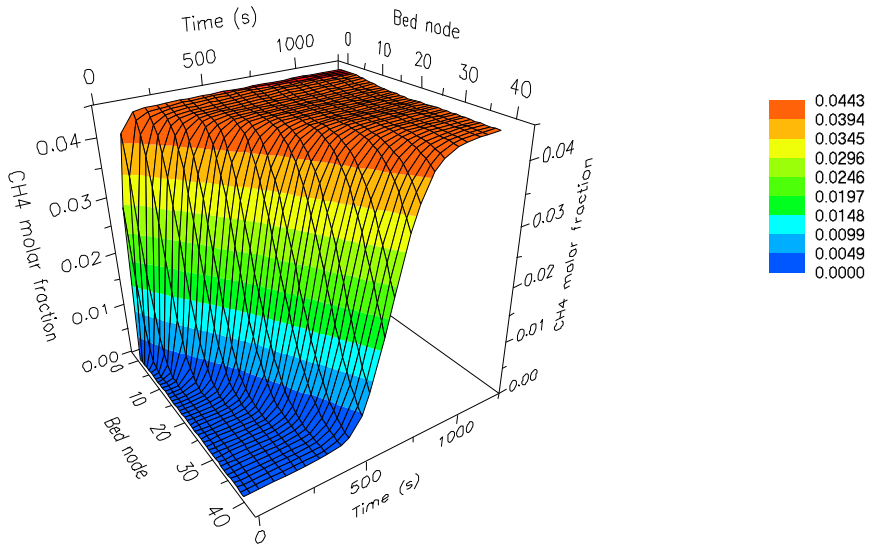

Figure 5. 8. Adsorption breakthrough curves for methane along the bed calculation nodes.

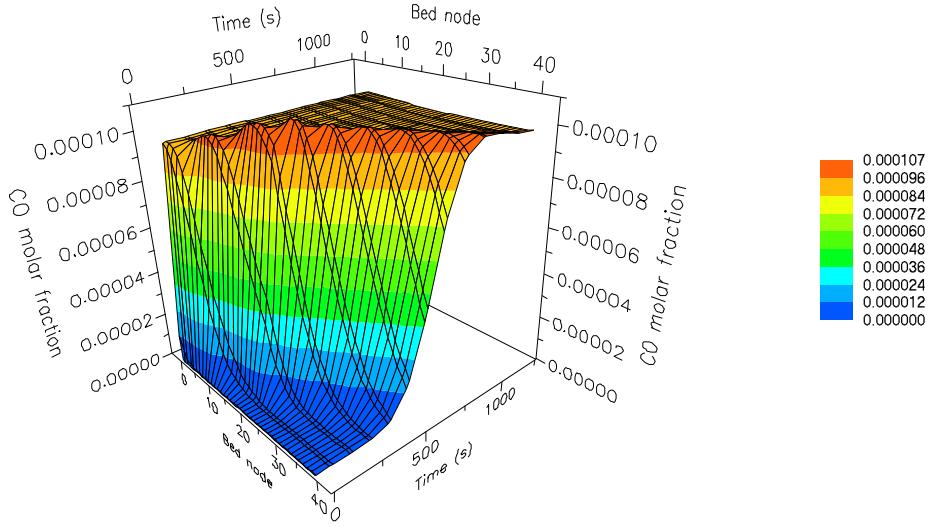

Figure 5. 9. Adsorption breakthrough curves for carbon monoxide along the bed calculation nodes.

Regarding hydrogen composition, it can be noted that at the first node of the adsorbent bed the composition for hydrogen rapidly decreases from a value of 1 (since the vessel was assumed to be initially filled with hydrogen) to _, corresponding to the feed molar fraction of hydrogen. As the gas phase flows through the adsorbent bed, the impurities get adsorbed whilst hydrogen passes through without practically being adsorbed. This happens until a certain point in time where the outlet composition, being the same as in the last note, starts to decay.

As for methane composition along the adsorbent bed, it is noted that at the initial simulation time and at the bed inlet (node 0) the molar fraction rapidly goes up to the feed methane fraction value, since the bed initially has no methane. The fraction of methane along the adsorbent bed stays at minimum values for a longer time as it approaches the product side of the vessel. The adsorbent agent saturates systematically, up until the last

calculation node is also affected and methane molar fraction starts to rapidly increase, contaminating the hydrogen product stream.

Until half of the adsorbent bed (node 0 to node 20) the molar fraction of carbon monoxide rapidly rose to the original feed composition values, but from half of the bed and on (corresponding to the zeolite layer) its molar fraction stays at lower values for longer time frames. Hence, its adsorption rate increases and thus it takes longer for the gas phase to show growth in the CO molar fraction. This is in accordance with the fact that carbon monoxide shows much stronger adsorption affinity with zeolite, resulting in being adsorbed into second layer considerably clearer than into the first layer of activated carbon (source already referenced, see number 13). As in the previous case with methane, as the gas flow approached the outlet of the bed, the available time without any carbon monoxide contamination at the gas outlet is broader.

The temperature was also plotted regarding the product outlet, which is shown in Figure 5. 10.

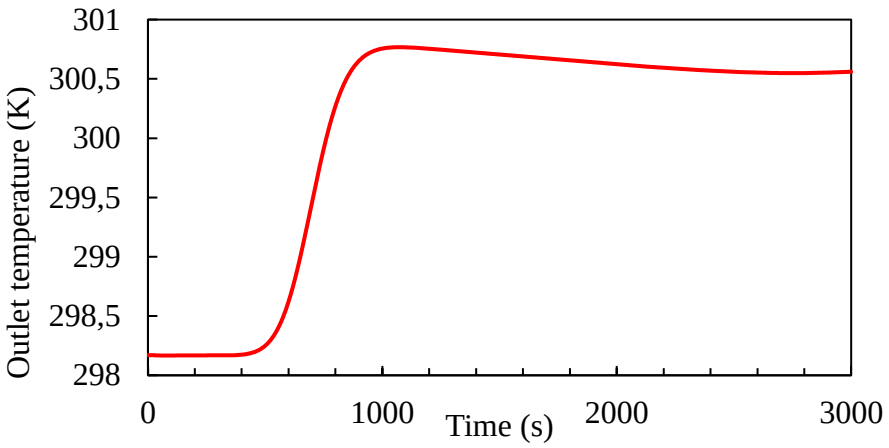

Figure 5. 10. Time evolution of temperature at the bed outlet.

The temperature of the gas at the product end of the bed stays constant at 25 ºC until simulation time = 500 s. Thereafter, it starts rising exponentially up to 300 K and later starts to decrease steadily, which matches with the previous patterns observed in the breakthrough curves (Figure 5. 4 to Figure 5. 6). This can be attributed to the fact that the front of impurities rapidly migrates to the outlet of the bed once the adsorbent has been saturated, contrary to the start of the run, where the adsorbent bed was clean (full of hydrogen) and the concentration front of impurities hadn't yet arrived to the outlet of the vessel.

However, as observed in Figure 5. 11, the temperature oscillation is much steeper at the feed end since the front of impurities is initially located at the earliest nodes. A significant decrease in the oscillation of temperature is observed as the gas advances through the bed towards its outlet. This is attributed firstly to the fact that the superficial gas velocity is higher at the feed end and systematically decreases as a consequence of the momentum balance within the bed, as seen in Figure 5. 12, especially at the earliest calculation iterations. It is also secondly attributed to the second half of the adsorbent bed corresponding to the zeolite layer. Both methane and carbon monoxide have higher heats of adsorption with respect to this agent, subsequently decreasing the temperature of the overall gas mixture.

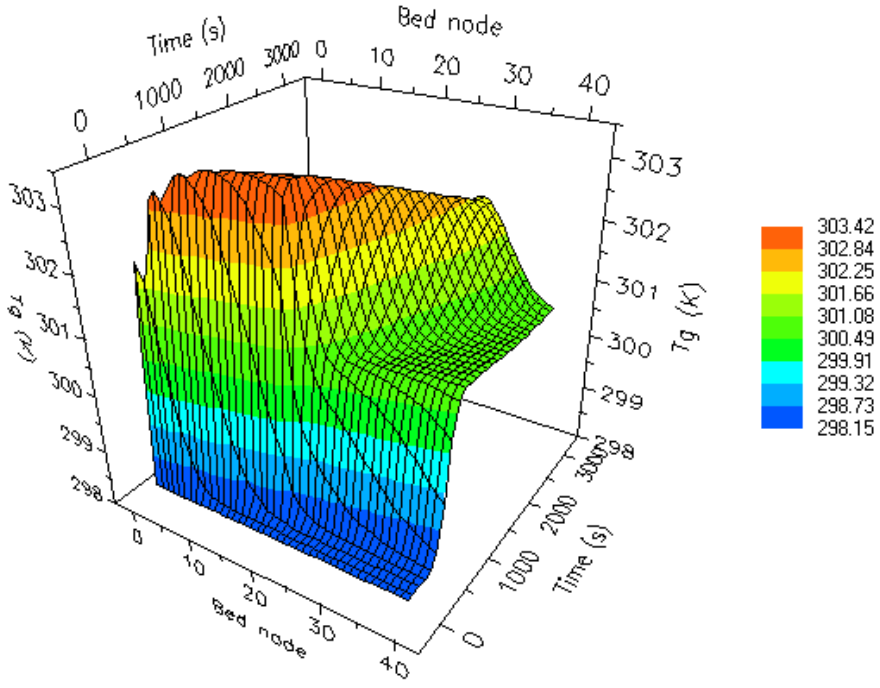

Figure 5. 11. Evolution of temperature with time and throughout the different bed nodes.

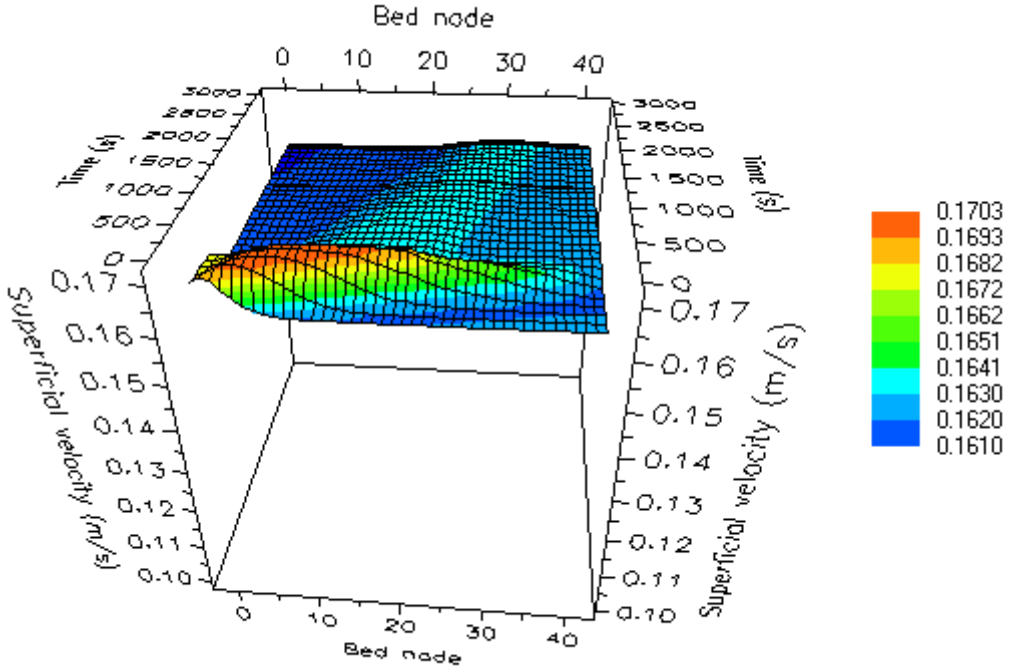

Figure 5. 12. Superficial gas velocity within the bed as a function time.

5.2. Base-case simulation results and model validation

The existing PSA unit was simulated accordingly to the described process parameters and constraints in section 4.3, the results of which were post-processed and are showed and examined herein.

The profile of the different vessel pressures as a function of time were plotted firstly with actual plant data using *PI Processbook*, which are shown in Figure 5. 13. The simulation results regarding the pressure oscillation are plotted as shown in Figure 5. 14.

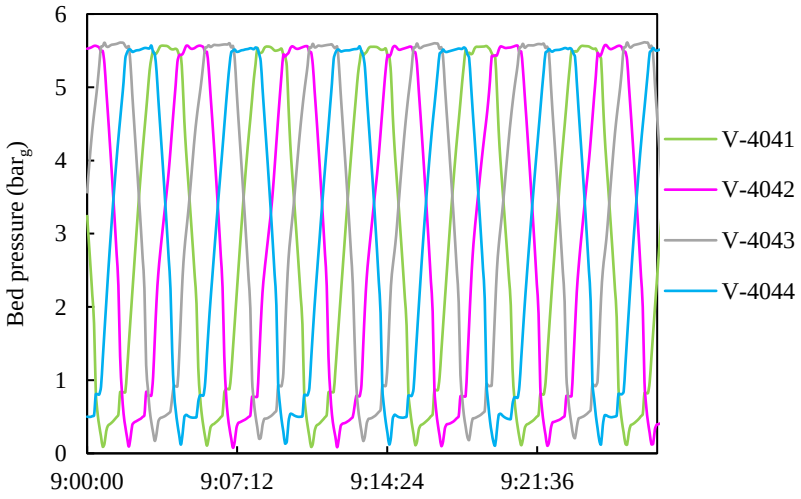

Figure 5. 13. Actual pressure measurements in the existing PSA system.

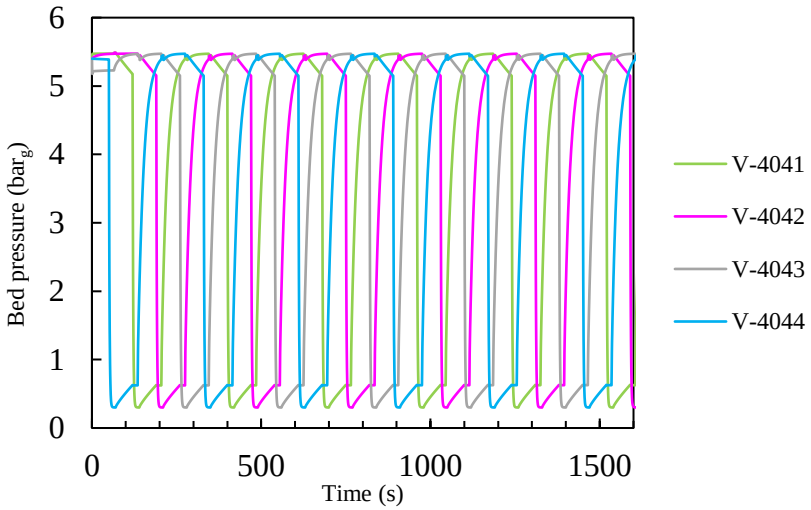

Figure 5. 14. Pressure pattern of the simulated four-bed PSA system.

The different pressure oscillations are evenly distributed throughout an arbitrary time slot, due to the cyclic nature of the process as was seen with the sequence schedule description. Although the pressure for both the starting and ending at each sequence step are correlated in time, the pattern of the different pressure gradients varies from the original monitoring to the one resulting from the simulation. This can be attributed to the approximations made through the bed model, combined with the influence of the estimated valve coefficients, which all adhere to a linear control form. The automatic valves that have a control action throughout any step involved in the actual PSA system sequence are equal percentage valves.

Figure 5. 15 shows a detailed pressure pattern of the bed corresponding to vessel V-4041, where the changes in pressure can be correlated to the applicable sequence step.

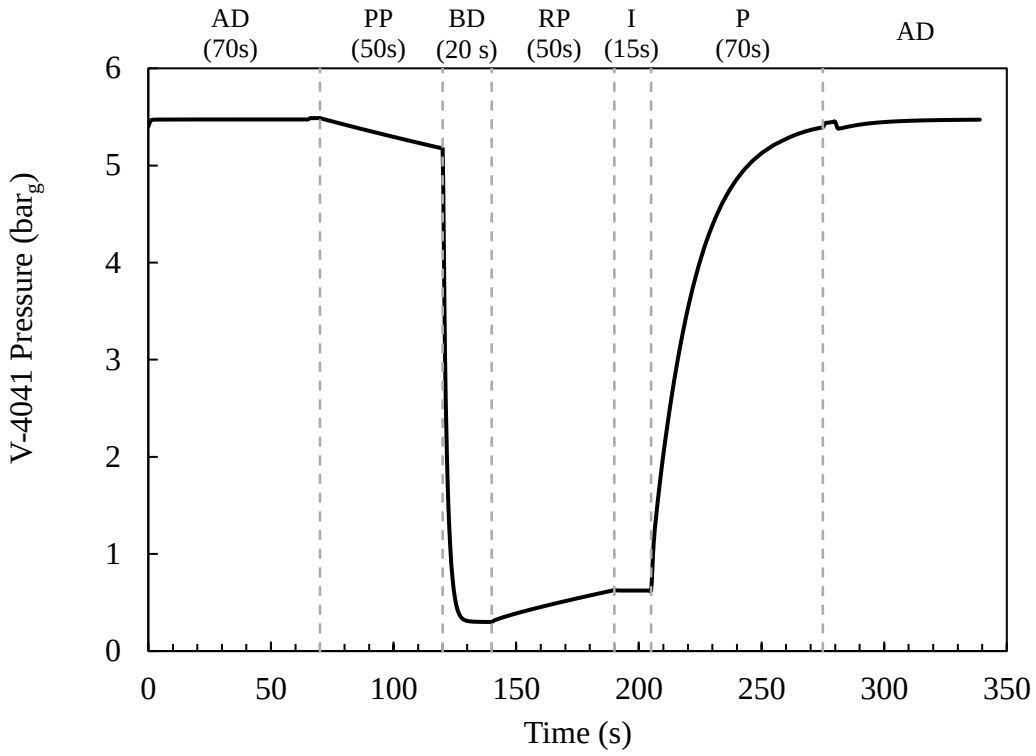

Figure 5. 15. Pressure pattern of a single adsorbent bed cycle in a four-bed system at 5 bar_g.

During the adsorption phase, the pressure at the column remains practically constant. Only a slight pressure increase is seen at the end of the adsorption phase, which corresponds to the adsorption overlap step. This is attributed to the instant when bed 3 is commencing its re-pressurize step, which is done by means of a controlled split stream from the hydrogen collector.

During the provide purge step, the bed depressurizes by opening its way towards the top manifold that connects with bed 4 without going into the hydrogen product collector.

The bed further depressurizes by closing the manifold communication and opening directly the bottom end towards the tail gas collector, reaching the lowest pressure available (tail gas) by completely opening the tail gas control valve.

With the aid of a purge stream from bed 2, which has now finished the adsorption phase to start depressurizing, the pressure can slightly increase whilst further migrating the front of impurities by means of the control action of the XV-40402 tail gas valve.

After the idle step, the bed starts re-pressurizing via a flow fraction of the hydrogen collector. Once the bed starts the adsorption phase again, a slight pressure peak is observed due to the overlapping of the adsorption phases from both V-4041 and V-4044, that is, XV-40414 opening a 100% instead of regulating. This also corresponds to the instant when bed 2 is commencing its re-pressurize step, which is done by means of a controlled split stream from the hydrogen collector.

The molar fraction evolution of the different components with time is shown from Figure 5. 16 to Figure 5. 19.

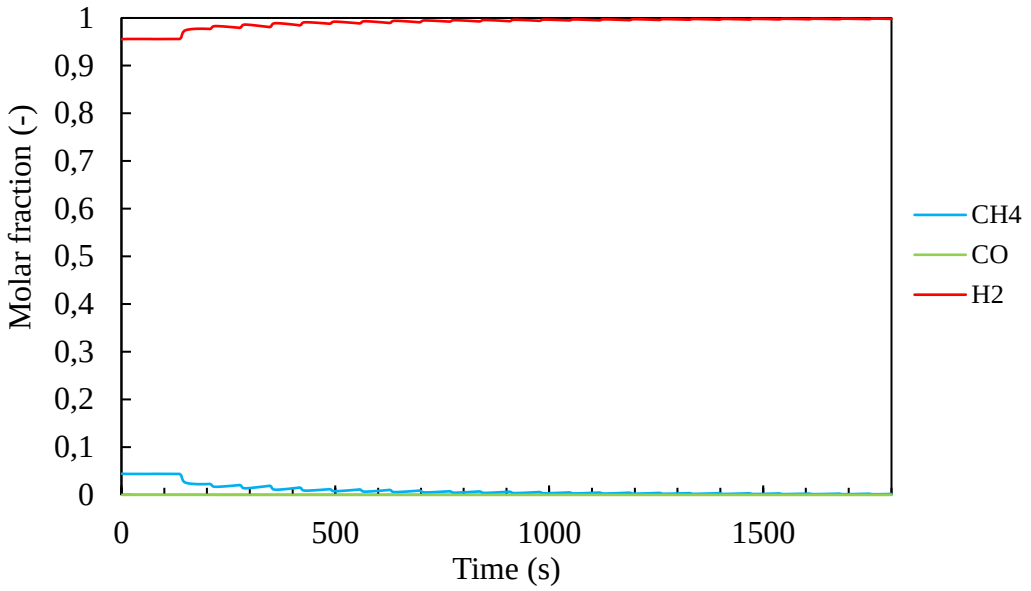

Figure 5. 16. General molar fraction evolution of the three components at the product outlet with the start of a run.

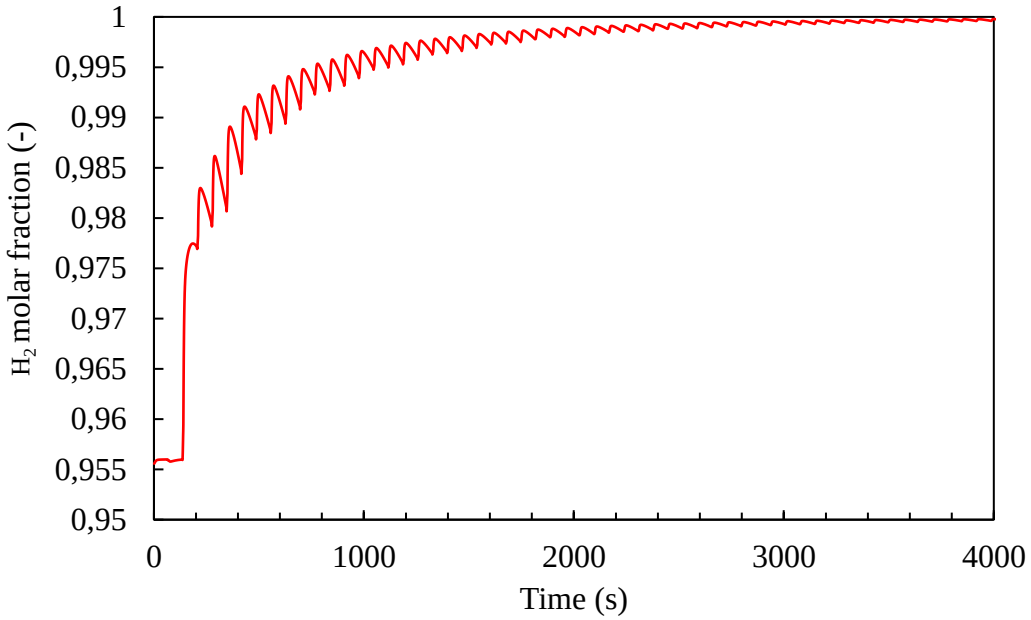

Figure 5. 17. Molar fraction evolution of hydrogen at the product outlet with the start of a run.

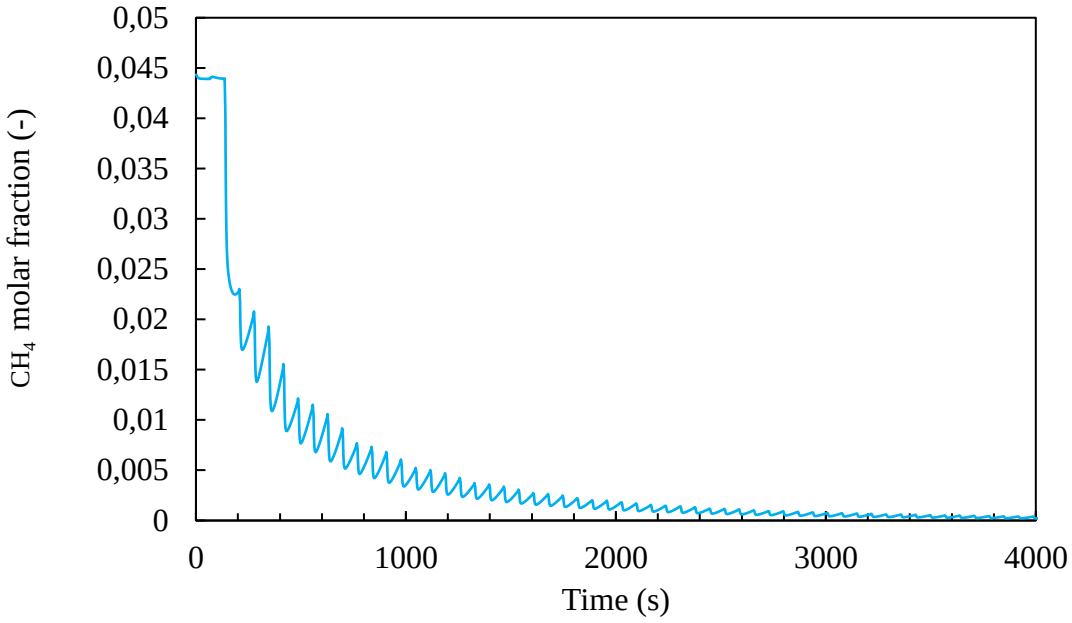

Figure 5. 18. Molar fraction evolution of methane at the product outlet with the start of a run.

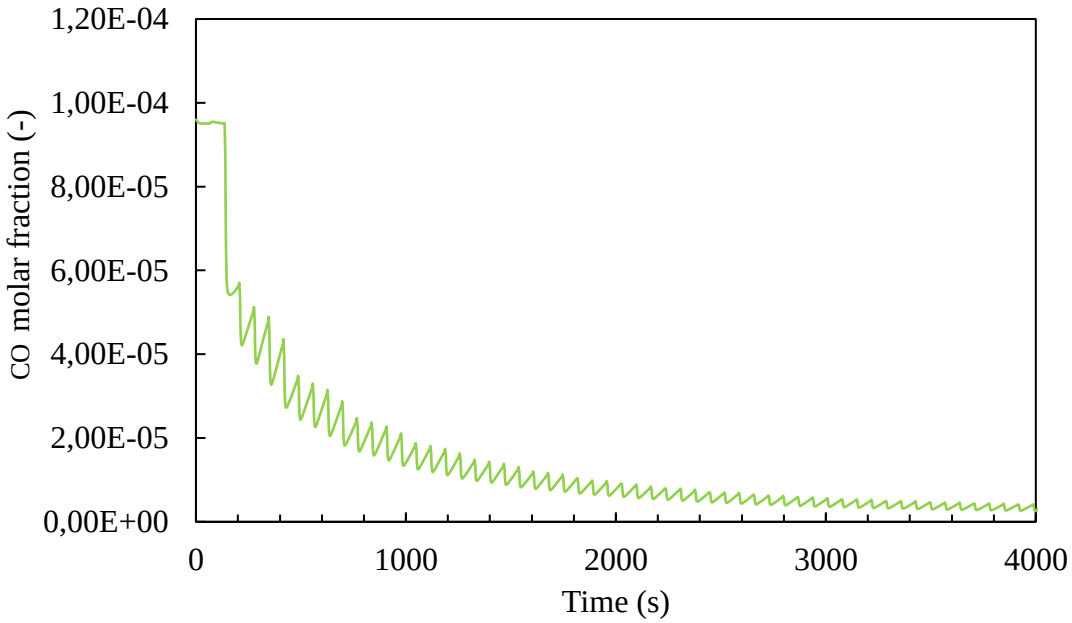

Figure 5. 19. Molar fraction evolution of carbon monoxide at the product outlet with the start of a run.

The molar fraction of hydrogen rapidly increases at the start of the run, easily reaching a value higher than 99% of purity during the second cycle. From then on, the purity rises more steadily, taking a considerable amount of simulation time to reach higher purities. A purity of _%, which would already be inside specification, is reached during cycle 12, at a simulation time of 3500s.

Regarding carbon monoxide, reaching the specification of less than _ ppm-v (or ppm molar, assuming it behaves as an ideal gas) takes a considerable amount of time in the simulation, as does on a start of run of the existing PSA unit. Concentration values for carbon monoxide were extracted from plant data by means of an existing CO analyser located at the product outlet of the PSA (Figure 5. 20) in order to compare it to the simulation results.

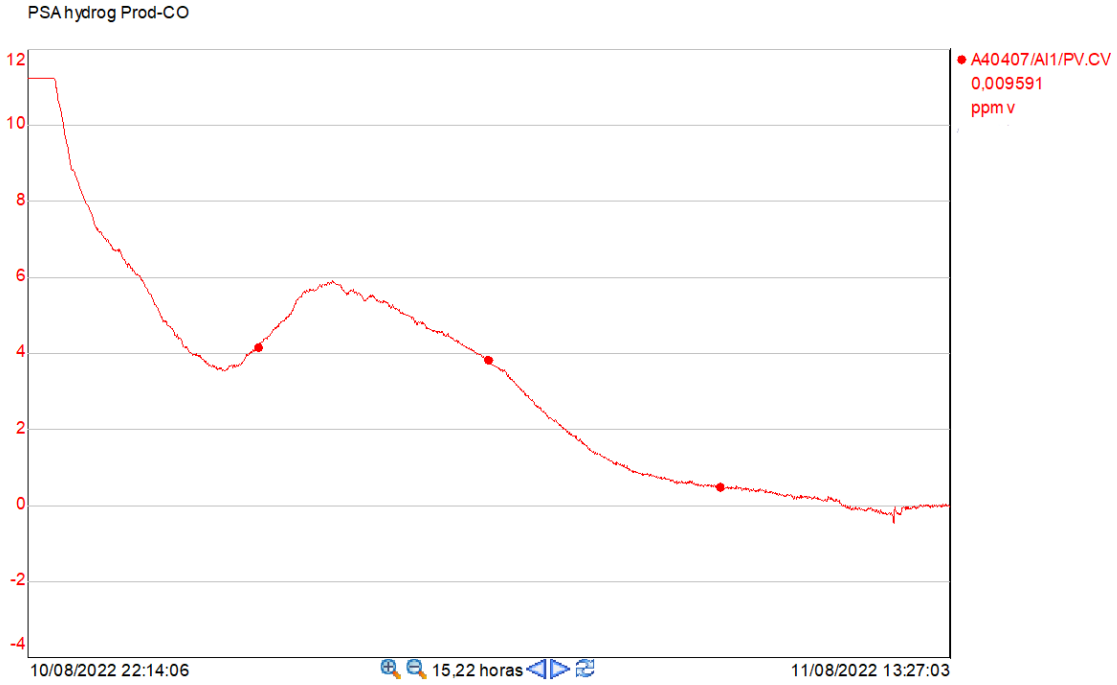

Figure 5. 20. Extracted plant data regarding carbon monoxide concentration at the product outlet of the actual PSA during the start of a run.

If the simulation carried out with *Aspen Adsorption* is left running for an extended time period, it can be observed that the molar concentration of CO at the product outlet decreases in a rather slow manner (see Figure 5. 21 and Figure 5. 22), as very low concentration magnitudes are being considered.

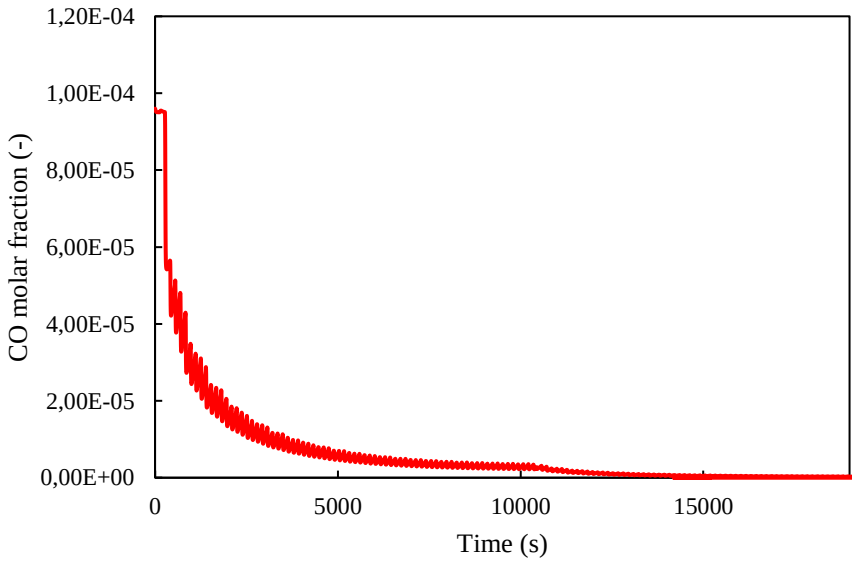

Figure 5. 21. Extended molar fraction evolution of carbon monoxide at the product outlet with the start of a run (I).

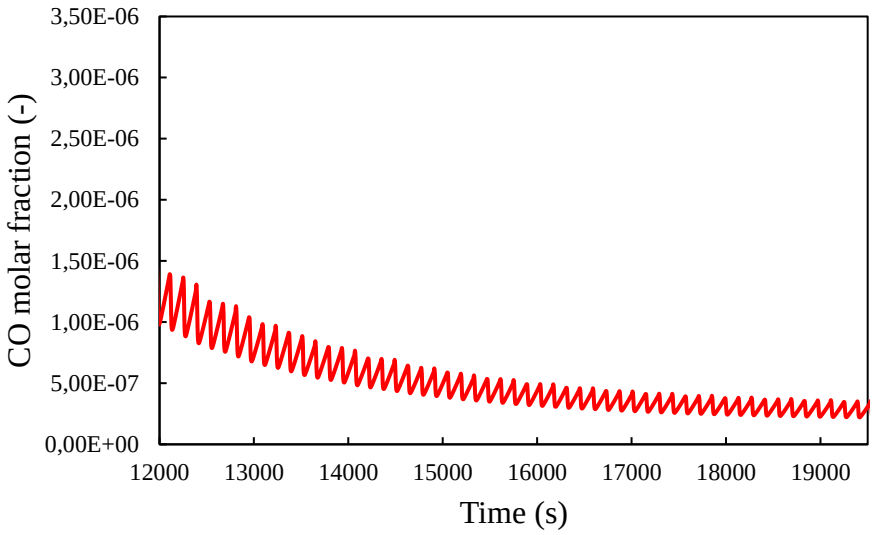

Figure 5. 22. Extended molar fraction evolution of carbon monoxide at the product outlet with the start of a run (II).

The specification of less than _ ppm-mol is reached from simulation time equal to _ seconds and forward, that is, six hours from the start of the run. The difference with respect to the real plant averaged data previously presented is that the molar concentration of carbon monoxide tends to increase during a certain period of time, which can be due to diverse process alterations in the first few hours of a start of run that influence the net gas inlet.

Regarding temperature at the product outlet, it follows a cyclic pattern accordingly with the sequence (which is a temperature behaviour typically observed in PSA systems, as supported by the already referenced source number 13) and it reaches a steady state relatively fast as seen in Figure 5. 23.

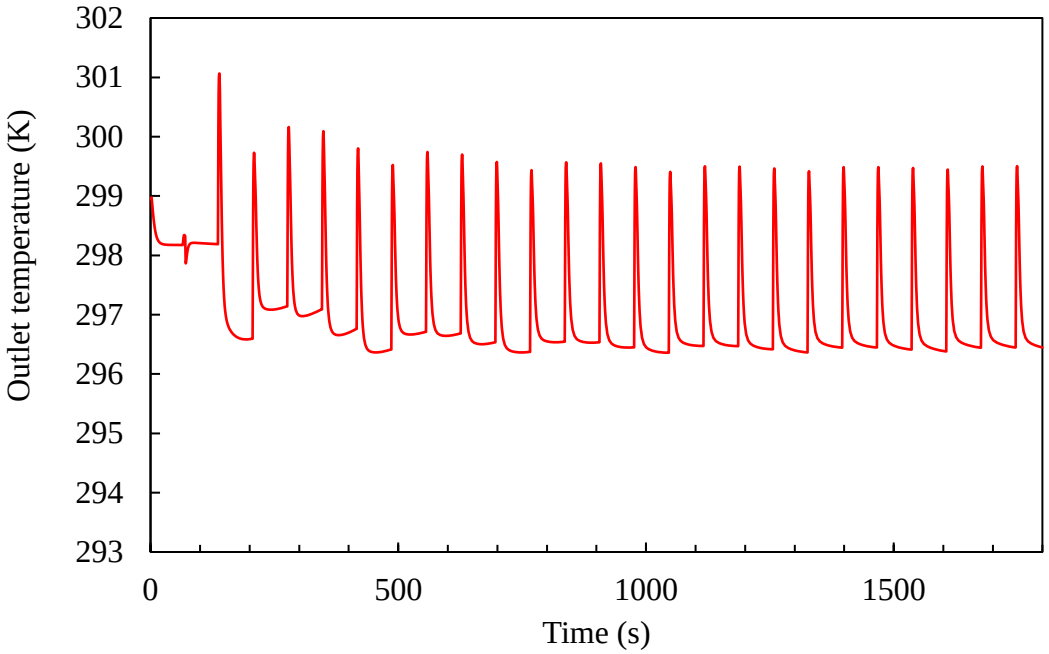

Figure 5. 23. Temperature oscillations monitored at the product outlet of the simulation.

Peaks at around 300 K are observed at cycle steps 3, 6, 9 and 12, which correspond to the adsorption overlap step, where two different beds have their XV-404X4 valve completely opened during 5s. Then, when a single bed undergoes the adsorption step, temperature decreases back to 293 K. This temperature difference is a consequence of the pressure peaks observed during the overlap step, as the pressure from the bed that has just finished re-pressurizing is slightly lower than that of the one that was already undergoing adsorption, subsequently leading to the sudden pressure equalization between the two beds.

Once the cyclic steady state is reached, the overall performance of the PSA can be evaluated by means of average flowrates as well as the present molar fractions in each of the main streams (net gas feed, hydrogen product and tail gas) as these barely change from one cycle to another. The withdrawn results from the simulation as well as the extracted data (normalized as described in section 2.1) corresponding to a feed peak of _ kg/h are shown in Table 5. 1.

Table 5. 1. Comparison between obtained results and actual process data.

	Simulation			Normalized plant data		
	Feed	Product	Tail gas	Feed	Product	Tail gas
Average Flowrate (kmol/h)	_	_	_	_	_	_
Molar composition						
Hydrogen (%)	_	_	_	_	_	_
Methane (%)	_	_	_	_	_	_
Carbon monoxide (ppm-mol)	_	_	_	_	_	_

The resulting hydrogen recovery is of _%, whilst the actual hydrogen recovery that was calculated with averaged data as mentioned in section 2.1 is of _% for the actual composition (also including ethane, propane, propylene, and ethylene) and with the normalised composition it is of _%. The obtained recovery is fairly close to the actual recovery that the system provides, given the different approximations made throughout the simulation. The valve coefficients were found to be one the most influencing parameters regarding the obtention of a steady product stream that is under specification. In addition, other parameters such as step times, valve activity and process parameters such as operating conditions were clearly defined based on the actual process, thus there was not an available range of choice.

5.3. Four bed system with an increased adsorption pressure

The four-bed system with an increased feed pressure to 30 bar_g had to be adjusted in order to reach a cyclic steady state in which the product would be under specification values whilst having a feed flowrate close to the one of reference, _ kmol/h. As seen in Figure 5. 24, the system's pressure shows a similar pattern to the one presented in the previous section at a decreased adsorption pressure, since the sequence itself wasn't changed but only values as step times and valve coefficients were adjusted.

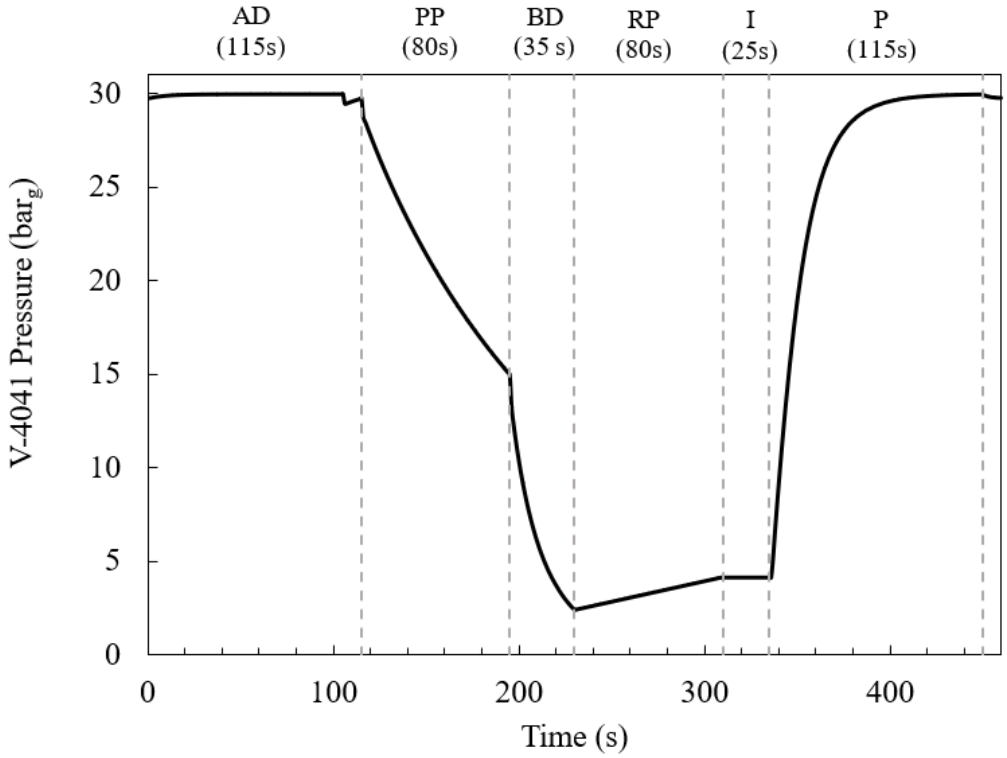

Figure 5. 24. Pressure pattern of a single adsorbent bed cycle in a four-bed system at 30 bar_g.

The adsorption overlap now presents a slight transient decrease in the collector pressure, as there is a re-pressurization start of bed 3 but also an adsorption bed phase start of bed 2, which leads to a slight de-stabilization of pressure before it is equalised.

The averaged results from the last executed cycle under a cyclic steady state are shown in Table 5. 2.

Table 5. 2. Simulation results for a 4-bed system at 30 bar_g.

	Feed	Product	Tail gas
Average Flowrate (kmol/h)	_	_	_
Molar composition			
Hydrogen (%)	_	_	_
Methane (%)	_	_	_
Carbon monoxide (ppm-mol)	_	_	_

Given the averaged flowrates and product compositions, hydrogen recovery is calculated resulting in a value of _%. Recovery has indeed considerably increased as a result of increasing the range of pressure oscillation, whilst purity was achieved to be maintained at averaged values higher than _% in hydrogen and a molar concentration regarding carbon monoxide under specification, plus at an average flowrate close to the reference value of _ kmol/h. This was done by properly adjusting the sequence with step times and valve coefficients.

Given the achieved results in the simulation, it can be concluded that providing the system with a wider pressure oscillation range by increasing the feed pressure can be a reasonable approach to improve the system's performance, as is hinted by adsorption theory.

Even so, a four bed system with an increased pressure ratio can further be optimised by having a zero idle time, which is reachable by adding one more pressure equalisation step per bed as explained in section 4.4, which implies adding an extra valve manifold that subsequently changes the sequence and the pressure pattern, resulting in the one shown in Figure 5. 25.

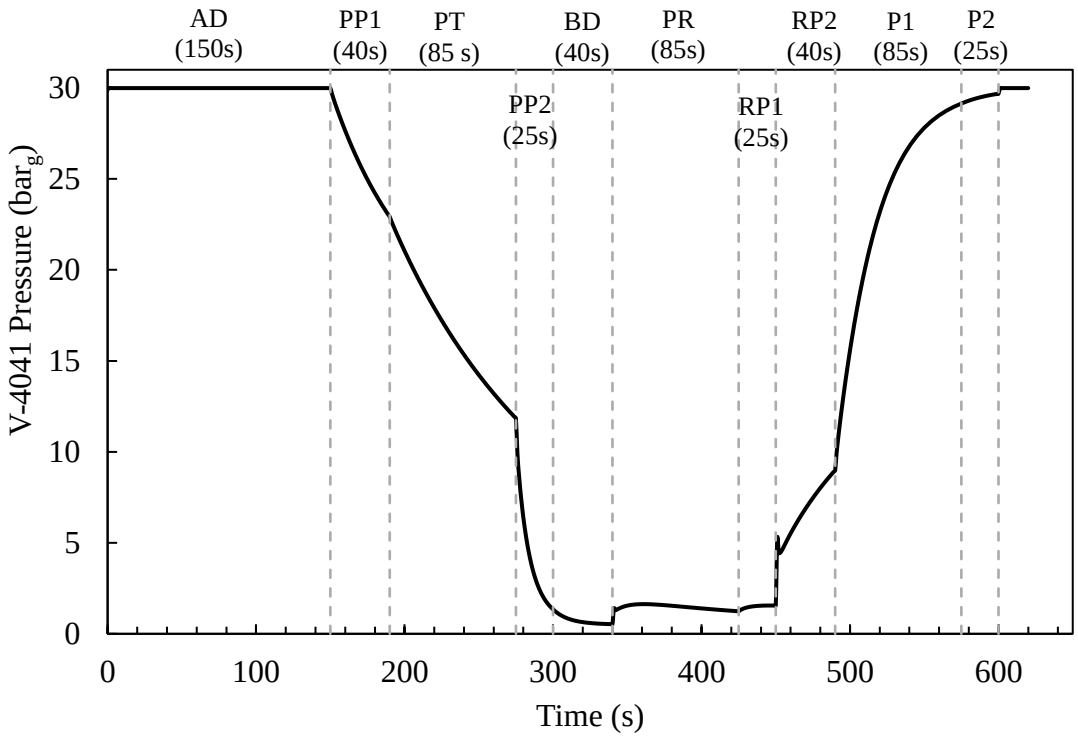

Figure 5. 25. Pressure pattern of a four-bed PSA with two equalisation steps at 30 bar_g.

As the previous case, once a cyclic steady state is considered to be reached (average values barely change from one cycle to another) the system's performance is evaluated. The extracted main results data from the simulation is shown in Table 5. 3.

Table 5. 3. Simulation results for a 4-bed and two pressure equalisation steps PSA at 30 bar_g.

	Feed	Product	Tail gas
Average Flowrate (kmol/h)	_	_	_
Molar composition			
Hydrogen (%)	_	_	_
Methane (%)	_	_	_
Carbon monoxide (ppm-mol)	_	_	_

As was made in all of the hypothetical simulations, both step times and valve coefficients were adjustable parameters that helped keeping the system under a stable feed flowrate and reaching a cyclic steady state with the product composition not surpassing the established requirement.

The obtained results now indicate an increased hydrogen recovery, which now takes the value of _%. Hence, it is reassured that adding pressure equalization steps in a four bed system can be an approach for enhancing the system's recovery, at an expense of a small decrease in the product quality but that it is still under specification. It must be taken into consideration that if no adjustments were made regarding step times and valve coefficient values with respect to the previous simulation, the difference in the product purity would be much broader, clearly seeing the hydrogen purity sensitivity with respect to recovery.

5.4. Six bed PSA at the original adsorption pressure

A six bed system is proposed as a way of further increasing pressure equalization steps to increase the system's hydrogen recovery.

It is initially considered under the current feed pressure, which corresponds to a rather moderate pressure oscillation. In this case, the range of adjustment was observed to be much narrower regarding valve coefficients and sequence step times, as there easily appeared convergence issues. It was attributed to the system having a reduced pressure range in relation to the number of steps that the bed was being forced to undergo in a single cycle.

The pressure profile is shown in Figure 5. 26. It can be seen that it was sufficient with the increased number of pressure equalization steps for a bed to reach back the adsorption pressure, thus the re-pressurization steps were undergone at practically the same pressure as in the adsorption phase. This hinted that the sequence was not optimal for a system with a limited pressure oscillation range, as the re-pressurization steps were not taken advantage of, hence the number of pressure equalization steps seemed to result too large for the defined system.

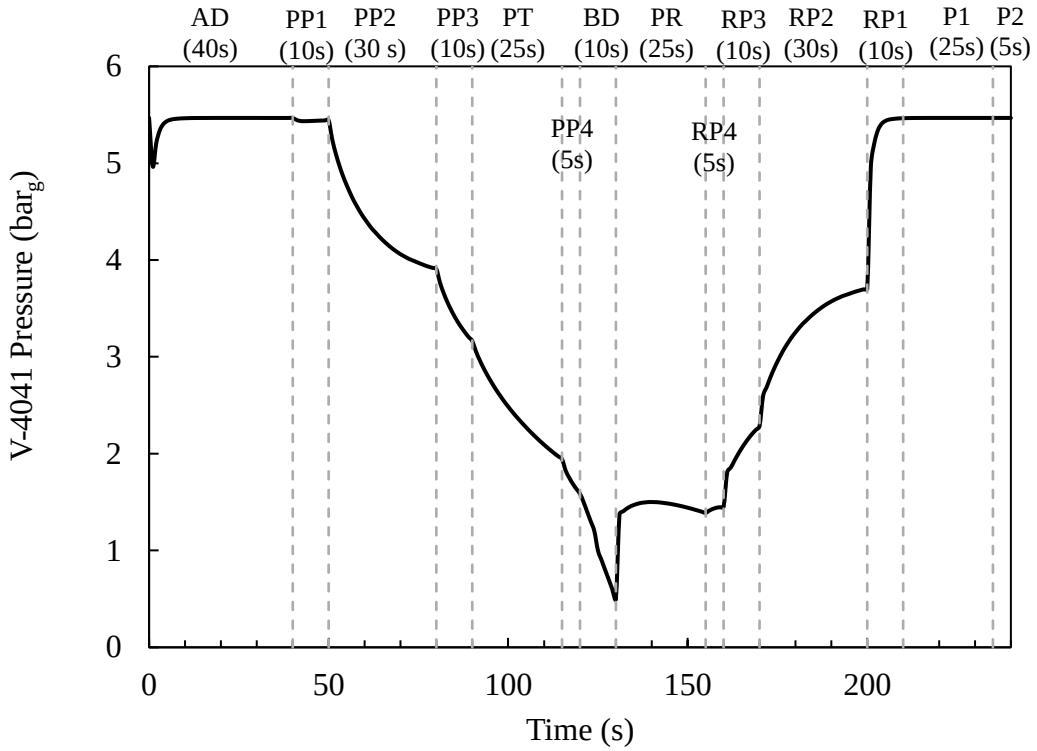

Figure 5. 26. Pressure pattern of a six-bed PSA at 5,5 bar_g.

The obtained average values from the achieved cyclic steady state of the simulation are shown in Table 5. 4.

Table 5. 4. Simulation results for a 6-bed PSA at 5,5 bar_g.

	Feed	Product	Tail gas
Average Flowrate (kmol/h)	_	_	_
Molar composition			
Hydrogen (%)	_	_	_
Methane (%)	_	_	_
Carbon monoxide (ppm-mol)	_	_	_

The obtained results indicate a hydrogen recovery of _%. This can be considered as a rather small improvement from that of the base-case, so it can be concluded that incorporating a system of six beds is more profitable when the pressure oscillation is wider rather than settling to the original adsorption pressure.

For lower pressure ratios between the feed and the tail gas than 10 and having a feed flowrate lower to 5000 Nm^3/h (which is the case, at around _ Nm^3/h), it was already foreseen with the recommendations from UOP that a system with 6 beds is not worth arranging if nor the pressure ratio between the feed and the tail gas nor the feed flowrate are increased in the current system.

According to UOP, a small capacity PSA can be not that worth to increase from a 4-bed to 6-bed system as the cost increases with pressure equalization steps in exchange to a small recovery gain (See referenced source number 2).

5.5. Six bed PSA at an increased adsorption pressure

The six-bed system is then tested with an increased feed pressure to tail gas pressure ratio. The pressure now follows a pattern as the one shown in Figure 5. 27, where it can be deduced that the sequence with four equalization step pairs per bed is better fit when the system has a larger pressure oscillation.

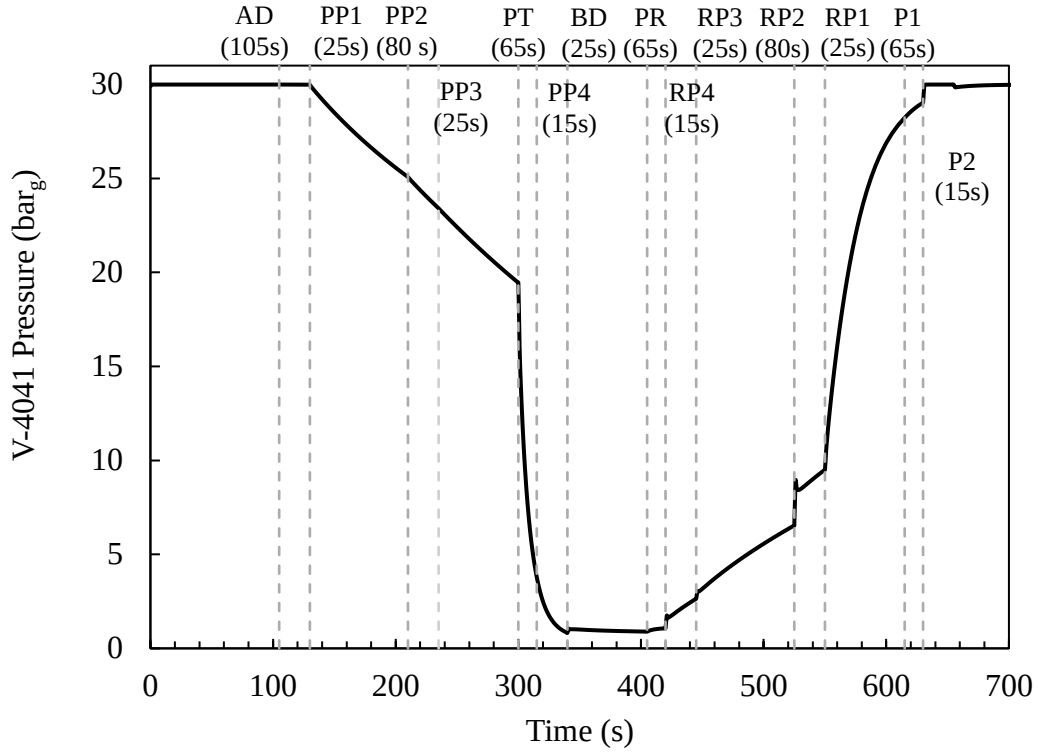

Figure 5. 27. Pressure pattern of a six-bed PSA at 30 barg.

Once the simulation reaches a cyclic steady state and the average values barely change from one cycle to another, the main simulation results are extracted and these match the values presented in Table 5. 5.

Table 5. 5. Simulation results for a 6-bed PSA at 30 bar_g.

	Feed	Product	Tail gas
Average Flowrate (kmol/h)	_	_	_
Molar composition			
Hydrogen (%)	_	_	_
Methane (%)	_	_	_
Carbon monoxide (ppm-mol)	_	_	_

The results show that a hydrogen recovery of _% is achievable once the cyclic steady state is reached. The system was once again adjusted via the trial and error of different cycle step times and valve coefficient values, with the aim of achieving a cyclic steady

state with a feed flowrate close to the reference value of _ kmol/h whilst also having the product composition values under the specification restrictions imposed.

There would exist a much more noticeable purity expense at the product if no adjustments were made regarding the process constraints and only the feed pressure was changed, as an increase in recovery would cause a decrease in hydrogen purity. Typically, a recovery increase equivalent to 1% would signify an increase in the key impurity component of 100 ppm, according to UOP (Source previously referenced source as number 2).

5.6. Summary of results

A summary of the obtained results regarding the PSA performance which is indicated by the hydrogen recovery is presented in Table 5. 6.

Table 5. 6. Summary of results regarding the performance of the different PSA simulations.

	H_2 recovery (%)
Current case (4 beds and 5,5 bar_g)	_
4 beds + Increased pressure (30 bar_g)	_
4 beds + Increased equalisations + Increased pressure (30 bar_g)	_
6 beds + 5,5 bar_g	_
6 beds + Increased Pressure	_

The obtained results will be used as the base for the revamping proposal in section 6.

6. REVAMP PROPOSAL OF THE EXISTING PSA UNIT

Since the maximum hydrogen recovery equivalent to _% was achieved (with also product composition that is under the required specification) by means of a simulation with an increased adsorption pressure up to 30 bar_g in addition to a system with six adsorbent beds, it is considered to be the most worth revamp approach for the problem at hand.

The revamp then implies the subsequent process sequence and control system modification, together with the addition of a compressor at the net gas feed that allows for it to reach the adsorption operating pressure of 30 bar_g. There is also the addition of the two additional adsorbent vessels, plus the piping modifications necessary for the arrangement of the six-bed PSA system. Although the Tail gas pressure is kept at the original plant's operation value, both the composition and the flowrate of the stream are different, consequently its compressor needs to be validated (which brings pressure back up to a value of 3,5 bar_g, according to the plant's needs).

Both the feed net gas and the tail gas compressors were assessed using *Aspen HYSYS*, by estimating the number of required compression steps, as well as the intercooling steps together with their respective duties.

The feed net gas compressor was estimated by taking into consideration the restriction that temperature must not exceed the temperature of 130 ºC, which is a reference value taken from other compression equipment in the plant and establishes a limit intended for the mechanical preservation of materials.

The starting base pressure of the net gas feed stream is on 5,5 barg, and it has to be compressed up to a 30 barg pressure whilst maintaining a temperature of 25 ºC as is in the case of the current inlet to the PSA unit.

Taking this into consideration, the arranged system in Aspen HYSYS consists in two compressing units and a heat exchanger after each one of them, which act as intercoolers by means of the available cooling water in the plant (found under the average conditions of 25 ºC and 3,8 barg) coming from the cooling towers. The reference regarding maximum temperature difference of cooling water is of 35 ºC.

Under the reference feed flowrate of _ kmol/h and with the normalized composition for the project, the results provided by the software regarding both the feed compressor and its necessary intercoolers are presented in Table 6. 1 and Table 6. 2, respectively.

Table 6. 1. Net gas feed compressor process specifications.

	Inlet (First stage)	Outlet (First stage)	Inlet (Second stage)	Outlet (Second stage)
C_p/C_v	1,41	1,40	1,41	1,40
Temperature (ºC)	25	130	25	120
Pressure (bar_g)	5,5	13,7	13,7	30,0
Molecular weight	2,64			
Mass Flow (kg/h)	_			
Volumetric flow, inlet (m^3/h)	_		_	
Stage duty (MW)	0,4236		0,3835	

Table 6. 2. Net gas feed intercoolers process specifications.

	Intercooler after first compressor stage		Intercooler after second compressor stage	
	Inlet	Outlet	Inlet	Outlet
Temperature, water (ºC)	25	60	25	60
Temperature, process (ºC)	130	25	120	25
Water pressure (bar_g)	3,8			
Water flowrate (m^3/h)	10,0		9,1	
Duty (MW)	0,4239		0,3840	

The tail gas compressor was estimated with the same approach, although it is an equipment that already exists in order to provide it at a pressure of 3,5 bar_g and a temperature equivalent to 20 ºC, according to the plant's needs. The main purpose is to estimate the differences in energy duties with respect to the base-case due to the flowrate and composition changes. These changes will also be of importance when estimating the economic viability of the project, since the heating value of the tail gas will most likely decrease in the new scenario and thus there will be a necessary supply of natural gas to compensate the loss of fuel gas that is used back in the plant's process.

The results regarding the new tail gas compressor process parameters as well as its necessary intercoolers are presented in Table 6. 3 and Table 6. 4, respectively.

Table 6. 3. Process specifications for the tail gas compressor after the PSA revamping.

	Inlet (First stage)	Outlet (First stage)	Inlet (Second stage)	Outlet (Second stage)
Cp/Cv	1,37	1,35	1,37	1,36
Temperature (ºC)	25	130	40	88
Pressure (bar_g)	0,3	2,1	2,0	3,5
Molecular weight	6,04			
Mass Flow (kg/h)				
Volumetric flow, inlet (m^3/h)				
Duty (kW)	71		32	

Table 6. 4. Tail gas intercoolers process specifications after the PSA revamping.

	Intercooler after first compressor stage		Intercooler after second compressor stage	
	Inlet	Outlet	Inlet	Outlet
Temperature, water (ºC)	25	60	25	60
Temperature, process (ºC)	130	40	88	20
Water pressure (bar_g)	3,8			
Water flowrate (m^3/h)	1,4		1,1	
Duty (kW)	61		45	

The tail gas compressor was also simulated for the base-case results previously presented in section 5.2. This is done for both evaluating the heating value of the resulting stream in order to compare the losses in the revamping case, and also for validating that the results are consistent with the existing compressor despite of the composition approximations made throughout the project.

The results obtained regarding both the tail gas compressor process parameters as well as the needed intercoolers for each stage are presented in Table 6. 5 and Table 6. 6, respectively.

Table 6. 5. Estimated process specifications for the tail gas compressor before the PSA revamping.

	Inlet (First stage)	Outlet (First stage)	Inlet (Second stage)	Outlet (Second stage)
Cp/Cv	1,40	1,38	1,39	1,39
Temperature (ºC)	25	130	40	90
Pressure (bar_g)	0,3	2,0	2,0	3,5
Molecular weight	3,83			
Mass Flow (kg/h)				
Volumetric flow, inlet (m^3/h)				
Duty (kW)	200		95	

Table 6. 6. Estimated tail gas intercoolers for the tail gas compressor before the PSA revamping.

	Intercooler after first compressor stage		Intercooler after second compressor stage	
	Inlet	Outlet	Inlet	Outlet
Temperature, water (ºC)	25	60	25	60
Temperature, process (ºC)	130	40	90	20
Water pressure (bar_g)	3,8			
Water flowrate (m^3/h)	4,1		3,1	
Duty (kW)	123		95	

The modified PSA unit Process Flow Diagram according to the proposed revamp is presented in Figure 6. 1.

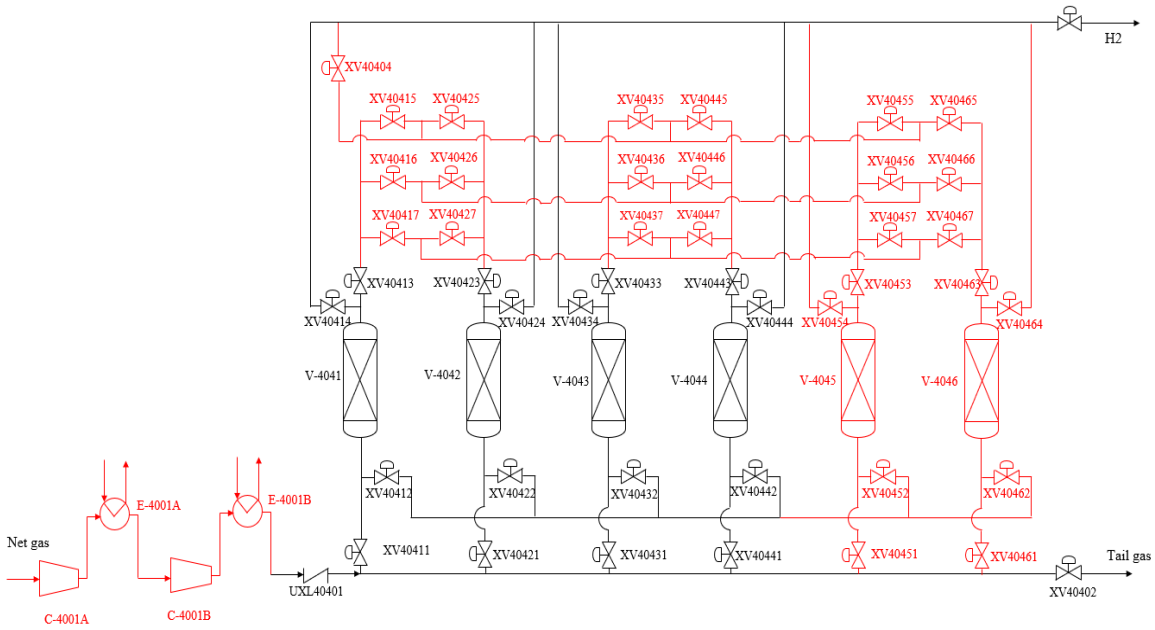

Figure 6. 1. Simplified Process Flow Diagram of the revamp proposal.

The current tail gas compressor's main motor, according to the specification data sheets, is of _ kW, whilst the calculated duty in the tail gas compressor is 295 kW. After reviewing the technical data of the existing tail gas compressor (located downstream of XV-40402), it is reassured that it can operate under the new duty conditions and volumetric flowrate.

The lower heating value of the tail gas is also evaluated for the later economic viability assessment. It is used instead of the higher heating value since the former excludes the vaporization energy of water, constituting a more restrictive case. The resulting LHV for the tail gas stream in the revamped PSA case is of _MJ/kg, whilst the one for the base-case tail gas stream is of _MJ/kg. Since the tail gas mass flowrate is also decreased in the

case of the revamped PSA, the difference with respect to the current fuel generation bets broader, corresponding to _MW.

6.1. Economic assessment

The estimation of the investment was made using the software *ESTIMADE™ plus*, as it is the case with feasibility studies (± 30% accuracy using the method of conceptual quantities) carried out within the company's both group and site engineering departments.

The software works for quantity-based cost estimations by applying different estimating modules according to the equipment type, materials and working conditions with an intrinsic database, conceptually generating quantities based on an equipment list. It can be used for both small capital projects and modifications up to large capital projects.

The investment cost breakdown using the *ESTIMADE™ plus* tool is shown in Table 6. 7.

Table 6. 7. Estimated investment cost breakdown for the revamp project.

	Estimated cost (€)	Percentage from total investment	Percentage from direct plant costs
Civil, structural and auxiliary work	304000	3,5	5,9
Insulation and painting	57000	0,7	1,1
Machines and equipment	3102000	35,5	60,5
Expediting	30000	0,3	0,6
Plant piping	140000	1,6	2,7
Electrical primary system	57000	0,7	1,1
Instrumentation and DCS hard and software	375000	4,3	7,3
Installation for D-L*	450000	5,1	8,8
Temporary construction facilities, scaffolding, etc.	360000	4,1	7,0
Installation labour, construction indirects and management	250000	2,9	4,9
Direct plant costs	**5125000**	**58,6**	**100,0**
Engineering	1700000	19,4	
Expense items (material & labor) and miscellaneous	52000	0,6	
Spare parts	90000	1,0	
Adsorbent material	125000	1,4	
Permits, fees and insurance, taxes, capitalized interest	94000	1,1	
Contingency	1560000	17,8	
Total project amount	**8746000**	**100,0**	

* Subgroups in installation labour according to internal classification, see Appendix C.2.

Once the investment cost has been estimated, the economic viability of the revamp project will be compared both to the current situation provided by the unit and the preliminary project involving the commission of an entirely new PSA unit with an increased capacity.

The energy cost is considered to be of _€/kWh, the supplied natural gas cost as a consequence of the heating value loss via the tail gas stream is of _€/GJ, an intake of _€/GJ is considered for an exported fraction of the TG stream, and the primarily set price to the purified hydrogen product is of _€/kg. The price to pay for CO_2 emissions is considered to be of _€/ton. The increase of the yearly maintenance cost is considered as 2% of the total inversion cost.

Taking these constraints into account, the viability and earnings comparison of the three possibilities is shown in Table 6. 8.

Table 6. 8. Economic feasibility comparison summary.

	Current PSA	Revamped PSA	PSA by Honeywell UOP
Feed to PSA (t/h)	_	_	_
H_2 produced (t/h)	_	_	_
Internal H_2 duty (t/h)	_	_	_
H_2 exported (t/h)	_	_	_
Sales H_2 (M€/y)	_	_	_
Total tail gas flowrate (ton/h)	_	_	_
Exported Tail gas (ton/h)	_	_	_
Tail gas intake (M€/y)	**0,24**	**0,21**	
Internally used tail gas power (GJ/h)	_	_	
Difference with current situation (GJ/h)	_	_	_
Natural Gas supply to cover the difference (ton/h)	_	_	_
Imported Natural Gas (M€/y)	**0,00**	**1,96**	**5,35**
CO_2 equivalent (ton/h)	_	_	_
CO_2 emission cost (M€/y)	**0,00**	**1,21**	**3,31**
Total power required (MW)	_	_	_
Power supply difference (M€/y)	**0,00**	**1,58**	**12,35**
Increase of maintenance cost (M€/y)	**0,00**	**0,18**	**0,70**
Earnings (M€/y)	_	_	_
Investment (M€)	**0,00**	**8,75**	**35,00**
Payback (y)	_	_	_

As seen in the previous summary table, differences with respect to the current case were taken into consideration regarding energy consumptions as well as available heating value from the tail gas stream, whose difference has to be supplied with natural gas. This subsequently leads to an additional cost due to CO_2 emissions.

The earnings are increased by roughly _ million euros per year with the proposed revamp. It has to be taken into account that the feed correlates the one from the current case, so it is a considerable improvement since the PSA's capacity is the same. The revamp proposal can be upscaled in order to produce an increase in yearly earnings, but with the current plant configuration an increased feed to the PSA is not a realistic approach.

However, in the case of the proposed preliminary project by Honeywell UOP, it involves an increased capacity PSA. This in turn implies several modifications not only

in the PSA section, but throughout numerous sections of the overall plant's process, which is why the PSA is allowed to produce more hydrogen and the conceptual project estimates a much larger investment cost. Both projects (revamping case and commission of a new PSA) have a payback period of _, although in the case of the proposed revamping it would take _ more.

7. CONCLUSIONS

It was possible to understand, model and simulate the dynamic operation of a Pressure Swing Adsorption unit, by reason of an exhausted real process data collection and normalisation with the help and training from the production department of the company, a thorough research involving detailed information about PSA processes via different studies and adsorption theory bibliography, and finally a mostly self-taught utilization of the *Aspen Adsorption* software, which has demonstrated to have a remarkable potential for the dynamic simulation of diverse types of adsorption processes, as elaborate as they are.

The simulations allowed to test to what extent hydrogen can be recovered without producing a hydrogen stream out of specification requirements. An upper limit of hydrogen recovery was encountered for each of the different approaches:

- The simulation of the existing PSA unit under current plant conditions and constraints allowed the recovery of a _% of the total fed hydrogen.
- The simulation of the existing PSA unit with an increased adsorption pressure up to 30 bar_g and a maintained desorption pressure down to 0,3 bar_g allowed the recovery of the _% of the total fed hydrogen.
- The simulation of the existing PSA unit but with the addition of an extra pressure equalisation step in the sequence allowed the recovery of the _% of the fed hydrogen.
- The simulation of a six-bed PSA unit was tested at both 5,5 bar_g and 30 bar_g of adsorption pressure, recovering the _% and the _% of the total hydrogen fed into the unit, respectively.

A six-bed PSA unit operating under 30 bar_g was considered the most attractive approach, for which an economic estimation was made considering the necessary new equipment with the subsequent re-programming and other costs such as civil and engineering works.

The net earnings throughout a year taking into consideration the estimations made was primarily evaluated, as well as the payback period. It was concluded that recovering the most part of hydrogen represents a feasible business opportunity for the company.

The overall work carried out as described in the present document is also advantageous for the plant to test different possibilities involving hydrogen recovery optimisation with the existing PSA unit, as well as the evaluation of different future potentials since there is a focus towards a strategy that allows the plant to make hydrogen a main product in addition to propylene in the future, for which there currently exist preliminary project proposals.

The current PSA unit simulation model can be used as a preliminary tool for limit testing that cannot be carried out live under the continuous plant operation, but further improvements can be done by testing several other parameters and approaches. The present model was based upon the premise that the layering would not be changed since the last loading procedure was carried out in August 2020, but in the case of future adsorbent loading procedures, other possibilities could be previously tested regarding different layering ratios. In addition, the model can be further refined by also considering radial gradients in both material and energy balances (that is, a 2D component instead of 1D). An automatic purity control can also be considered as a next approach possibility, as this allows to automatically adjust step times according to impurity analysis in the product (Patented by *UOP*). Other improvements can be done, such as including the tail gas mixing drum in the simulation to minimize flowrate and composition variations, and also modelling isotherms for the other present components in the net gas.

8. REFERENCES

[1] The Linde Group. Hydrogen Recovery by Pressure Swing Adsorption. 23942.ICS.0816

[2] J. Stöcker, M. Whysall and G.C. Miller. *30 Years of PSA Technology for Hydrogen Purification*. (1998)

[3] Yavary, M., Ebrahim, H.A., The effect of the number of pressure equalisation steps on the performance of pressure swing adsorption process. Chemical Engineering and Processing, 87 (2015) 35-44.

[4] T. Löfqvist, K. Sokas, J. Delsing, Speed of sound measurements in gas-mixtures at varying composition using an ultrasonic gas flow meter with silicon based transducers. Paper presented at International Conference on Flow Measurement, Groningen, Netherlands (2003)

[5] 2000 Dresser Industries, Inc., Masoneilan Control Valve Sizing Handbook. Bulletin OZ1000. 7/00.

[6] Aspen Technology Inc., *Adsorption Reference Guide*, Adsim Version 2004.1. Cambridge, MA, USA (April 2005).

[7] J. Jee, M. Kim, C. Lee. Adsorption Characteristics of Hydrogen Mixtures in a Layered Bed: Binary, Ternary and Five-Component Mixtures. *Ind. Eng. Chem. Res.* **2001**, *40*, 868-878.

[8] Wakao, N., T. Funazkri. Effect of Fluid Dispersion Coefficients on Particle-to-Fluid Mass Transfer Coefficients in Packed Beds. Chem. Eng. Sci. 33, 1375 (1978).

[9] Bird, R. B., Stewart, W. E., & Lightfoot, E. N. *Transport phenomena*. New York (1960).

[10] Glueckauf, E. Formulae for diffusion into spheres and their application to chromatography. Theory of chromatography, Part 10. Atomic Energy Research Establishment, Harwell. 1955

[11] Ahn S, Your YW, Kim KH, Lee CH. Layered two- and four-bed PSA processes for H2 recovery from coal gas. *Chem. Eng. Sci.*, 2012;**68(1)**:413-23.

[12] Yang, J., Chang-Ha, L., and Chang, J.W. Separation of Hydrogen Mixtures by a Two-Bed Pressure Swing Adsorption Process Using Zeolite 5A

[13] J. Xiao, Y. Peng, P. Bénard, R. Chahine. Thermal effects on breakthrough curves of pressure swing adsorption for hydrogen purification. *International Journal of Hydrogen Energy.* 41(2016);8236-8245.

[14] The American Society of Mechanical Engineers. ASME Boiler & Pressure Vessel Code, Part II-Materials, Part D-Properties. (2019 Edition)

[15] Aspen Technology, Inc., Introduction to Aspen Adsorption. *AspenTech Customer Education Manual*. Course nº ES288.071.07.

[16] Baksh et al., Pressure Swing Adsorption for the production of hydrogen. United States Patent, no. US 6,340,382 B1. (Jan 22, 2002)

[17] Baksh et al., Six bed Pressure Swing Adsorption process operating in normal and turndown modes. United States Patent, no. US 8,491,704 B2. (Jul 23, 2013)

APPENDICES

Contents

Appendix A. Actual project tasks duration

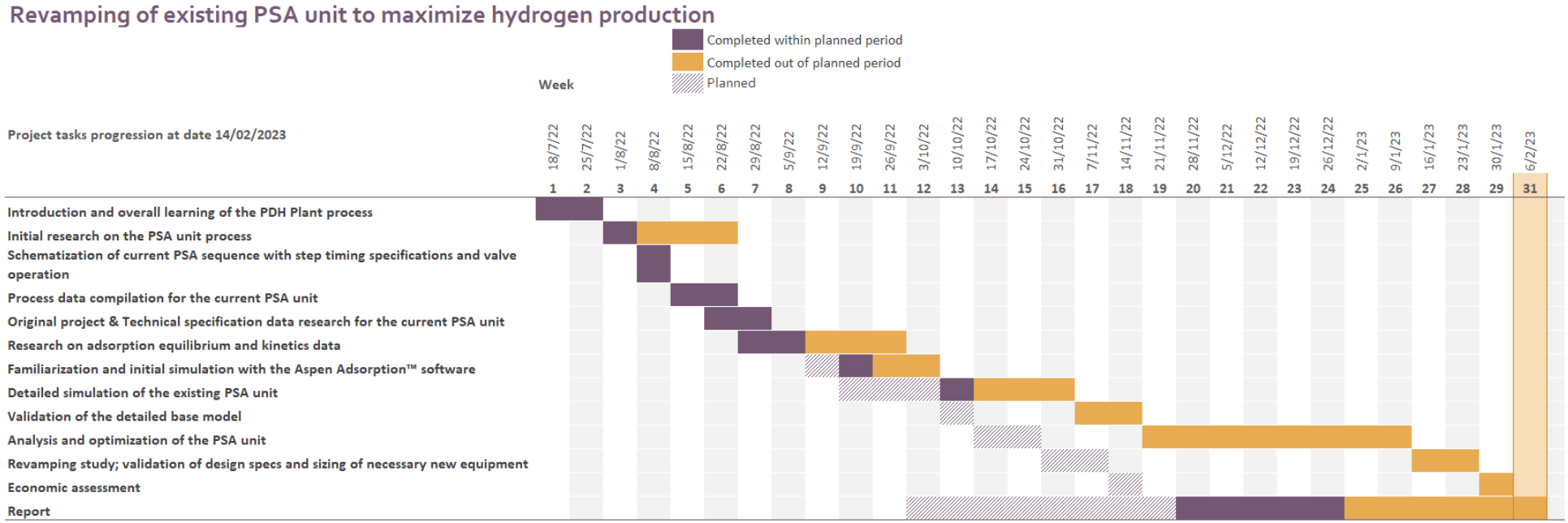

Appendix B. Actual PSA sequence schematized by Emerson

Steps	1	2	3	4	5	6	7	8	9	10	11	12	13	14	15	1
Phases	1			2				3				4				
Bed A	Adsorb XV40411 XV 40414 100%			Adsorb Overlap		Propurge XV40413 (U404X3_C) (100%)		Blowdown XV40412 (100%)		RecPurge XV40412 XV40413 (-35%)	Idle	Repress XV40414 (U404X4_C) Control				Ext Rep
Bed B	Repress XV40424 (U404X4_C) Control			Ext Rep		Adsorb XV40421 XV 40424 100%		Adsorb Overlap		Propurge XV40423 (U404X3_C) (100%)	Blowdown XV40422 (100%)			RecPurge XV40422 XV40423 (-35%)	Idle	
Bed C	Blowdown	RecPurge XV40432 XV40433 (-35%)	Idle	Repress XV40434 (U404X4_C) Control				Ext Rep		Adsorb XV40431 XV 40434 100%		Adsorb Overlap		Propurge XV40433 (U404X3_C) (100%)	Blowdown XV40432 (100%)	
Bed D	Adsorb overlap	Propurge XV40443 (U404X3_C) (100%)		Blowdown XV40442 (100%)		RecPurge XV40442 XV40443 (-35%)	Idle	Repress XV40444 (U404X4_C) Control				Ext Rep		Adsorb XV40441 XV40444 100%		

Appendix C. Additional Investment cost information

C.1. Actual investment cost output report using ESTIMADE™ plus

EstiMADE™plus (2022.4.1 IV/2022)
Cost estimation for changes and projects

Alpha-structure project

BASF
We create chemistry

Project title: Expansión PSA a 6 lechos
Job-Nummer: 0000
Project number:
Version:
Revision:
Final approval: 06.2023
Ready for startup: 07.2025

Group	Name	Default [EUR]	% von A-U	% von E	
A	Civil & structural, auxiliary work (material & labor)	104.365	1,2 %	3,4 %	
B	Insulation, painting, hvac etc, (material & labor)	57.033	0,7 %	1,8 %	
C	Moveable inventory (material)	0	0,0 %	0,0 %	
D	Packaged Units	0	0,0 %	0,0 %	
E	Machines & Equipment	3.101.983	35,9 %	100,0 %	
G	Utility Equipment	0	0,0 %	0,0 %	
Ex	Expediting	30.263	0,3 %		
H	Plant piping (material)	138.378	1,6 %	4,5 %	
I	Offsite piping (material)	0	0,0 %	0,0 %	
K	Electrical primary system (material)	56.554	0,7 %	1,8 %	
L	Electr./instrumentation (material), DCS (hard & software)	372.541	4,3 %	12,0 %	
M0	Installation for D-L	450.895	5,2 %	14,5 %	
M1	Temporary Construction Facilities, Scafolding, etc.	360.716	4,2 %	11,6 %	
M2	Installation labor, construction indirects, construction management	247.992	2,9 %	8,0 %	
A-M	**Direct plant costs**	**4.920.721**	**56,9 %**		
N	Engineering	1.903.520	22,0 %		
O	Expense Items (material & labor), miscellaneous	51.381	0,6 %		
S	Spare parts	89.499	0,0 %		is not summed up, as already included in individual groups
Cat	Catalysts	125.000	1,4 %		
T	Permits, fees & insurance, taxes, capitalized interest	94.317	1,1 %		
U	Contingency	1.557.426	18,0 %		
A-U	**Project amount**	**8.652.365**	**100,0 %**		

C.2. Installation labour subgroups D-L

All plant equipment (Group D) items, including special rigging, tools, shim plates, temporary supports.

All plant equipment (Group E) items, including special rigging, tools, shim plates, temporary supports.

All plant equipment (Group G) items, including special rigging, tools, shim plates, temporary supports.

INSTALLATION LABOR FOR PLANT PIPING (H) – Includes for the erection of all plant piping (Group H) systems. Includes all fabrication and erection of piping systems, hangers and supports, testing, X-rays, stress relieving, cleaning and pickling, and tie-ins. Also included is unloading, hauling, welder qualification, etc.

INSTALLATION LABOR FOR OFFSITE PIPING (I) – Includes for the erection of all plant piping (Group I) systems. Includes all fabrication and erection of piping systems, hangers and supports, testing, X-rays, stress relieving, cleaning and pickling, and tie-ins. Also included is unloading, hauling, welder qualification, etc.

INSTALLATION LABOR FOR ELECTRICAL (K) – Includes labour costs for the installation of all electrical items and systems on the project. Includes all installation activities for major electrical equipment, tray and channel systems, power and instrument wiring, lighting, supports, stands, terminations, hook-ups, etc. Also included in unloading, hauling, loop and continuity checks, and miscellaneous items.

INSTALLATION LABOR FOR INSTRUMENTS (L) – Includes labour costs for the installation of all instrument and control items or systems on the project. Includes all installation activities for the DCS control panel, instrument hardware and associated bulk materials, supports, stands, and air or process tubing. Also included is unloading, hauling, and testing.

Appendix D. Additional molar fraction evolution plots

D.1. Pressure increase with idle time

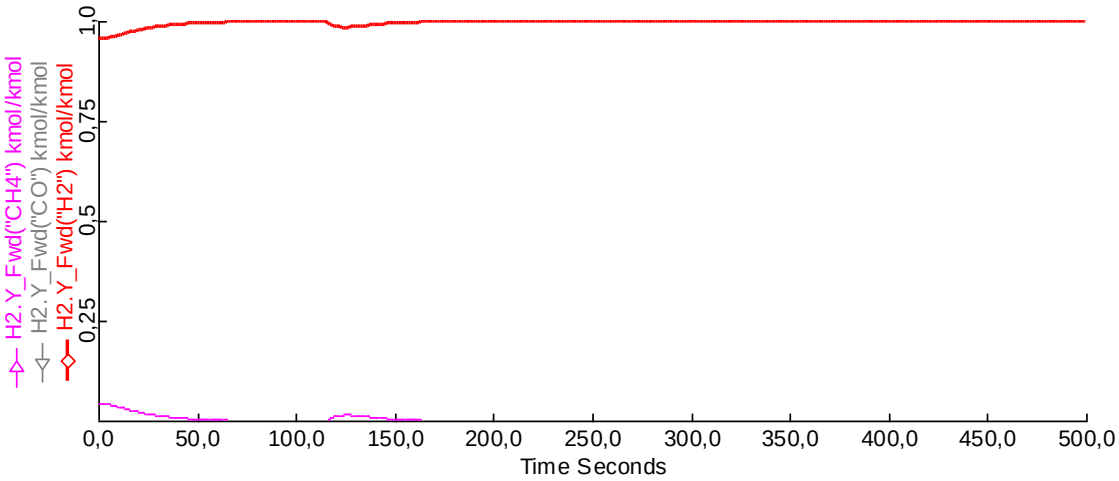

D.2. Pressure increase without idle time (additional pressure equalisation step)

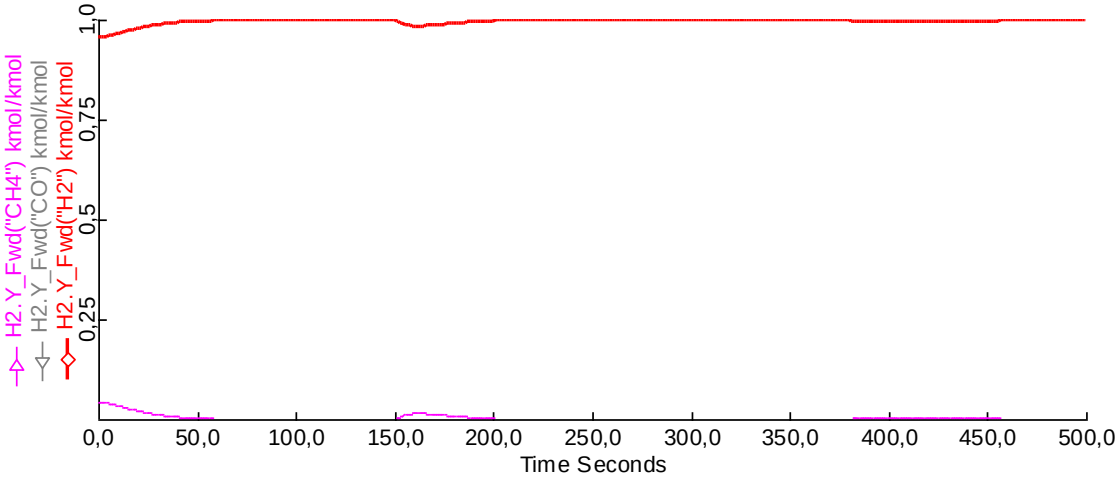

D.3. Six-bed PSA and increased pressure

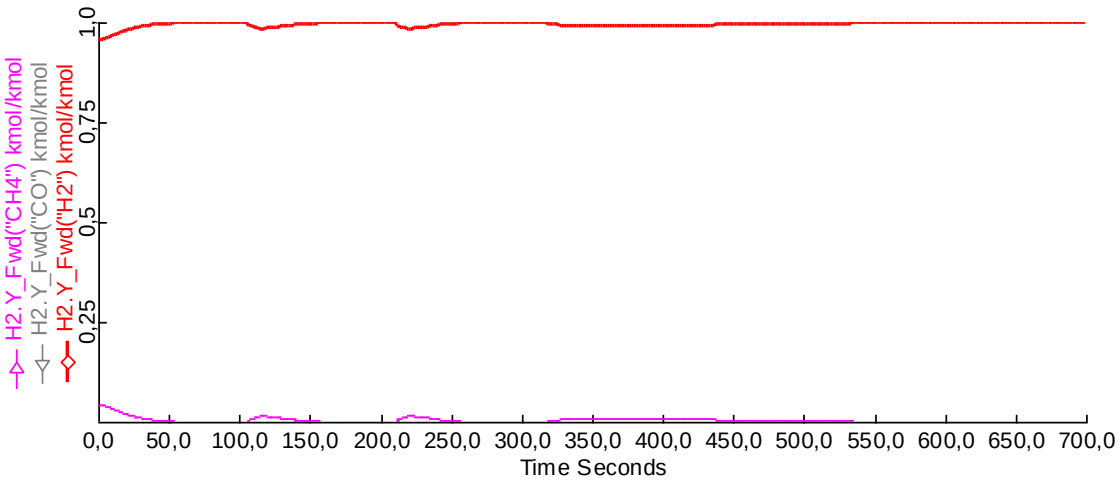

Appendix E. Actual loading of adsorbent material of a vessel in the current PSA unit

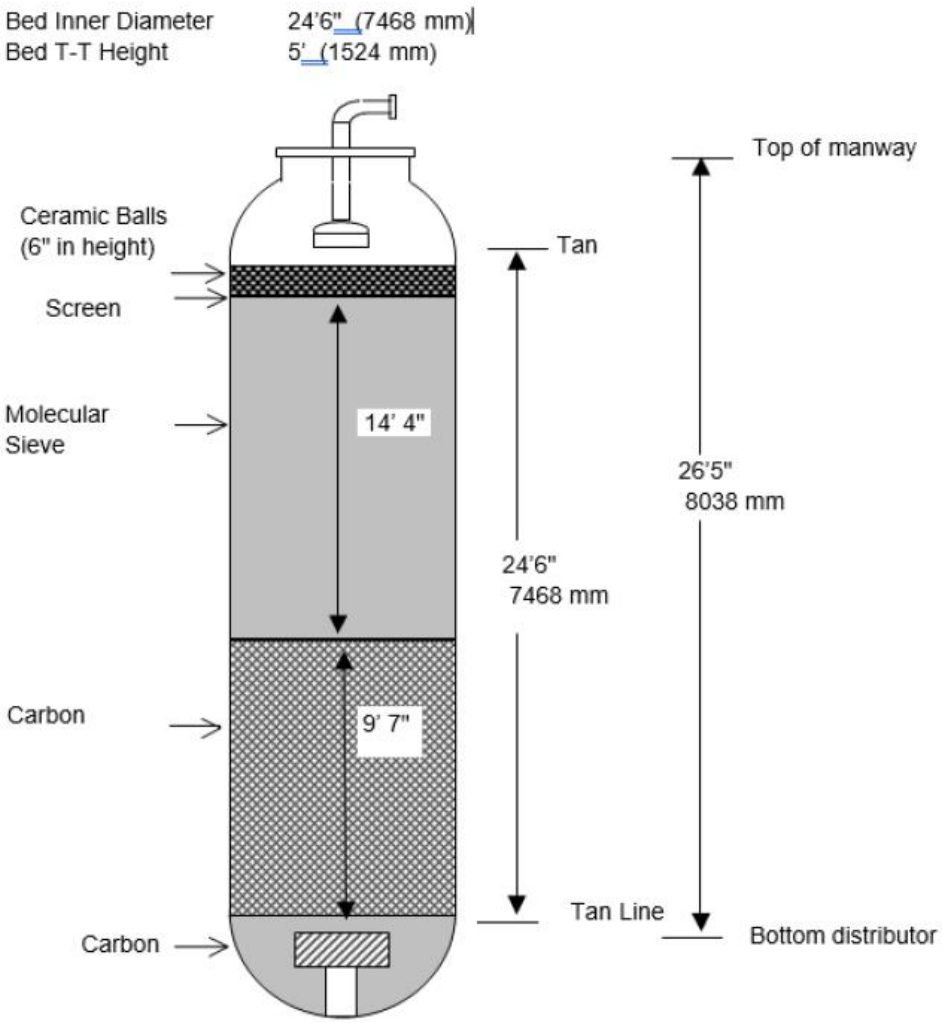

Appendix F. Self-evaluation Questionnaire

Degree Competences		Task in which you have observed the competence	Self evaluation [Rank 1 to 10]	Aspects to be improved
SPECIFIC COMPETENCES				
A1.1	Effectively apply knowledge of basic, scientific and technological materials pertaining to engineering.	Valve rating, Aspen adsorption simulations, Basic simulations in Aspen HYSYS	8	Improve knowledge and effectiveness when manipulating Aspen Adsorption software
A1.2	Design, execute and analyze experiments related to engineering	Aspen adsorption simulations, Basic simulations in Aspen HYSYS, basic material balances	8	Broaden the range of experiments carried out
A1.3	Be able to analyze and synthesize the continuous progress of products, processes, systems and services, whilst applying criteria of safety, economic viability, quality and environmental management. (G6)	Possible savings analysis carried out	8	Improve knowledge on economic assessments
A1.4	Know how to establish and develop mathematical models by using the appropriate software in order to provide the scientific and technological basis for the design of new products, processes, systems and services and for the optimization of existing ones. (G5)	Aspen Adsorption model approach	10	Further experiment with other possible models
A2.1	Be able to apply the scientific method and the principles of engineering and economics to formulate and solve complex problems that arise in processes, equipment, installations and services, in which the material undergoes changes to its composition, state or energy content, these changes being characteristic of industrial chemistry and other related sectors such as pharmacology, biotechnology, materials sciences, energy, food	Whole internship tasks carried out	8	Lack of experience. Improve self-dependent knowledge.

	and the environment. (G1)			
A2.2	Conceive, project, calculate and design processes, equipment, industrial installations and services in the field of chemical engineering and related industrial sectors in terms of quality, safety, economics, the rational and efficient use of natural resources and the conservation of the environment. (G2)	Economic assessment	8	Improve the economic estimation with in-depth detail
A2.3	Lead and technically and economically manage projects, installations, plants, companies and technological centres in the ambit of chemical engineering and related industrial sectors. (G3)	N/A		
A3.1	Apply knowledge of mathematics, physics, chemistry, biology and other natural sciences by means of study, experience, practice and critical reasoning in order to establish economically viable solutions for technical problems (I1).	Economic assessment	8	Improve knowledge and information basis on energy and/or supply costs
A3.2	Design and optimize products, processes, systems and services for the chemical industry on the basis of various areas of chemical engineering, including processes, transport, separation operations, and chemical, nuclear, elctrochemical and biochemical reactions engineering (I2).	Whole internship	8	Improve data analysis and treatment for more accurate results
A3.3	Conceptualize engineering models and apply innovative problems solving methods and appropriate IT applications to the design, simulation, optimization and control of processes and systems (I3).	Aspen Adsorption and HYSYS simulations	9	Integrate results in-between different simulation software
A3.4	Be able to solve unfamiliar and ill-defined problems by taking into account all possible	Whole master's thesis	10	Improve problem resolution timings

	solutions and selecting the most innovative. (I4)			
A3.5	Lead and supervise all types of installation, process, system and service in the different industrial areas related to chemical engineering (I5).	N/A		
A3.6	Design, construct and implement methods, processes and installations for the integrated management of waste, solids, liquids and gases, whilst also taking into account the impacts and risks of these products (I6).	N/A		
A4.1	Lead and organize companies and production and service systems by applying knowledge and abilities regarding industrial organization, commercial strategy, planning and logistics, mercantile and labour legislation, and financial and costs accounting (P1).	N/A		
A4.2	Lead and manage the organization of work and human resources by applying criteria regarding industrial safety, quality management, occupation risk prevention, sustainability and environmental management (P2).	N/A		
A4.3	Manage research, development and technological innovation whilst ensuring the transfer of technology and taking into account property and patent rights (P3).	Overall internship	9	Further research on metal sulfidation equilibria could have been carried out
A4.4	Adapt to structural changes in society caused by economic, energy or natural factors so as to be able to solve any resulting problems and to contribute technological solutions with a high commitment to sustainability (P4).	N/A		

A4.5	Lead and monitor the control of installations, processes, products, certification, auditing, verification, testing and reports (P5).	N/A		
A5.1	Carry out, present and defend (once all the curriculum credits have been obtained) an original individually produced piece of work before a university panel. The work will consist of a professional integrated Chemical Engineering project that synthesizes (TFM1)	Master's thesis project	9	Further testing and improvements could be done with an extended period of time
TRANSVERSAL COMPETENCES				
B1.1	Communicate and discuss proposals and conclusions in a clear and unambiguous manner in specialized and non-specialized multilingual forums (G9).	Consulting of doubts in different departments	8	Third-party companies could have been consulted. *Fundació URV* was momentarily consulted for the possibility of obtaining original isotherm models, but these lacked the necessary equipment.
B1.2	Adapt to changes and be able to apply new and advanced technologies and other important developments with initiative and entrepreneurial spirit. (G10)	Overall internship	8	Improve self-dependent knowledge to not depend on consulted doubts
B2.1	Lead and define multidisciplinary teams that are able to make technical changes and address management needs in national and international contexts. (G8)	N/A		
B3.1	Work in a team with responsibilities shared among multidisciplinary, multilingual and multicultural teams	Overall internship	9	Other departments that could have been consulted, such as economic/administrative
B4.1	Be able to learn autonomously in order to maintain and improve the competences pertaining to chemical engineering that enable continuous professional development. (G11)	Overall internship	10	Further improve knowledge on other problem approaches
B5.1	Carry out and lead the appropriate research, design and development of engineering solutions in new or little	Overall master's thesis	8	Further research on PSA functioning and improvements on proposed solutions can be done

	understood areas, whilst applying criteria of creativity, originality, innovation and technology transfer. (G4)			
B5.2	Bring together knowledge, make judgements and take decisions on the basis of incomplete or limited knowledge whilst taking into account the social and ethical responsibilities of professional practice. (G7)	N/A		
NUCLEAR COMPETENCES				
C1.1	Have an intermediate mastery of a foreign language, preferably English	Master's thesis in english	9	Vocabulary can be improved.
C1.2	Be advanced users of the information and communication technologies	Master's thesis project	9	Self-taught utilization of the software
C1.3	Be able to manage information and knowledge	Overall internship	8	Improve folder classification for working time optimisation
C1.4	Be able to express themselves correctly both orally and in writing in one of the two official languages of the URV	Meetings and consultations	9	Improve conciseness and technical vocabulary
C2.1	Be committed to ethics and social responsibility as citizens and professionals	N/A		
C2.2	Be able to define and develop their academic and professional project	Overall internship	8	Improve time optimisation with the next master's thesis project that will also be carried out within BSP

b) Evaluate the final master project and suggest improvements.

Key steps	**Evaluation [Mark 1 to 10]**	**Improvement proposed**
Selection/assignment of the project (dissemination, communication, assignment requirements...)	9	Improve the definition of objectives within an assigned project
Stay (welcome, length, relationship, follow-up made by the company...)	10	N/A
Follow-up made by URV tutor	10	N/A
Other aspects to be considered (which ones...)	N/A	N/A